Environmental Science & Technology

pubs.acs.org/est

Critical Review

A Tale of Two Foulants: The Coupling of Organic Fouling and Mineral Scaling in Membrane Desalination

Tiezheng Tong,* Xitong Liu,* Tianshu Li,* Shinyun Park, and Bridget Anger

Cite This: *Environ. Sci. Technol.* 2023, 57, 7129−7149

Read Online

ACCESS | Metrics & More | Article Recommendations

ABSTRACT: Membrane desalination that enables the harvesting of purified water from unconventional sources such as seawater, brackish groundwater, and wastewater has become indispensable to ensure sustainable freshwater supply in the context of a changing climate. However, the efficiency of membrane desalination is greatly constrained by organic fouling and mineral scaling. Although extensive studies have focused on understanding membrane fouling or scaling separately, organic foulants commonly coexist with inorganic scalants in the feedwaters of membrane desalination. Compared to individual fouling or scaling, combined fouling and scaling often exhibits different behaviors and is governed by foulant−scalant interactions, resembling more complex but practical scenarios than using feedwaters containing only organic foulants or inorganic scalants. In this critical review, we first summarize the performance of membrane desalination under combined fouling and scaling, involving mineral scales formed *via* both crystallization and polymerization. We then provide the state-of-the-art knowledge and characterization techniques pertaining to the molecular interactions between organic foulants and inorganic scalants, which alter the kinetics and thermodynamics of mineral nucleation as well as the deposition of mineral scales onto membrane surfaces. We further review the current efforts of mitigating combined fouling and scaling *via* membrane materials development and pretreatment. Finally, we provide prospects for future research needs that guide the design of more effective control strategies for combined fouling and scaling to improve the efficiency and resilience of membrane desalination for the treatment of feedwaters with complex compositions.

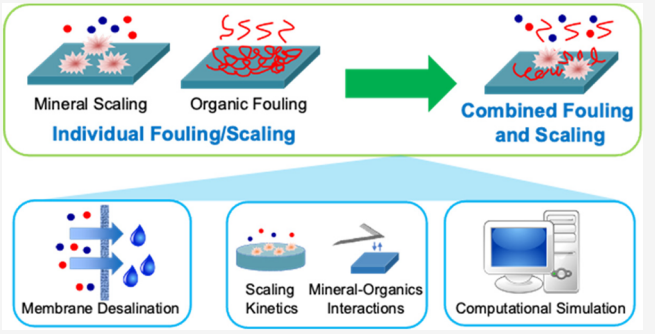

KEYWORDS: *membrane desalination, organic fouling, mineral scaling, mineral−organic interaction, fouling and scaling control*

1. INTRODUCTION

The dwindling freshwater resources due to climate change, anthropogenic pollution, and rising water demand in municipal, industrial, and agricultural sectors have resulted in four billion people facing water shortage globally.[1] For example, both the United States and China, the two largest economies globally, have suffered from severe droughts and heat waves in 2022,[2−4] with water stress imposing a pressing threat to regional economy, energy generation, as well as ecological and human health. To address the grand challenge of water scarcity, desalination technologies that enable harvesting of purified water from unconventional water sources, such as seawater, brackish groundwater, and wastewater, have become indispensable to augmenting freshwater supply beyond the hydrological cycle.[5−7]

Thanks to the development of membrane desalination technologies during the recent decades, a portfolio of technologies has been established for the treatment and reuse of unconventional water sources. Pressure-driven reverse osmosis (RO) and nanofiltration (NF) are currently the state-of-the-art desalination technologies due to their exceptional energy efficiency.[6,8] Although RO and NF are constrained by their salinity limit imposed by the maximum operating pressure,[9] other membrane technologies such as forward osmosis (FO) and membrane distillation (MD) are able to tolerate high salinity and treat hypersaline wastewater toward minimal or zero liquid discharge (MLD or ZLD).[10−12] However, the performance of membrane desalination is greatly constrained by membrane fouling and scaling, which decrease efficiency and increase both the cost and energy consumption of desalination systems. Organic fouling takes place when the organic matter in the feedwater adsorbs on the membrane surface. Due to the ubiquitous presence of organic substances

Received: January 15, 2023
Revised: April 17, 2023
Accepted: April 18, 2023
Published: April 27, 2023

https://doi.org/10.1021/acs.est.3c00414
Environ. Sci. Technol. 2023, 57, 7129−7149

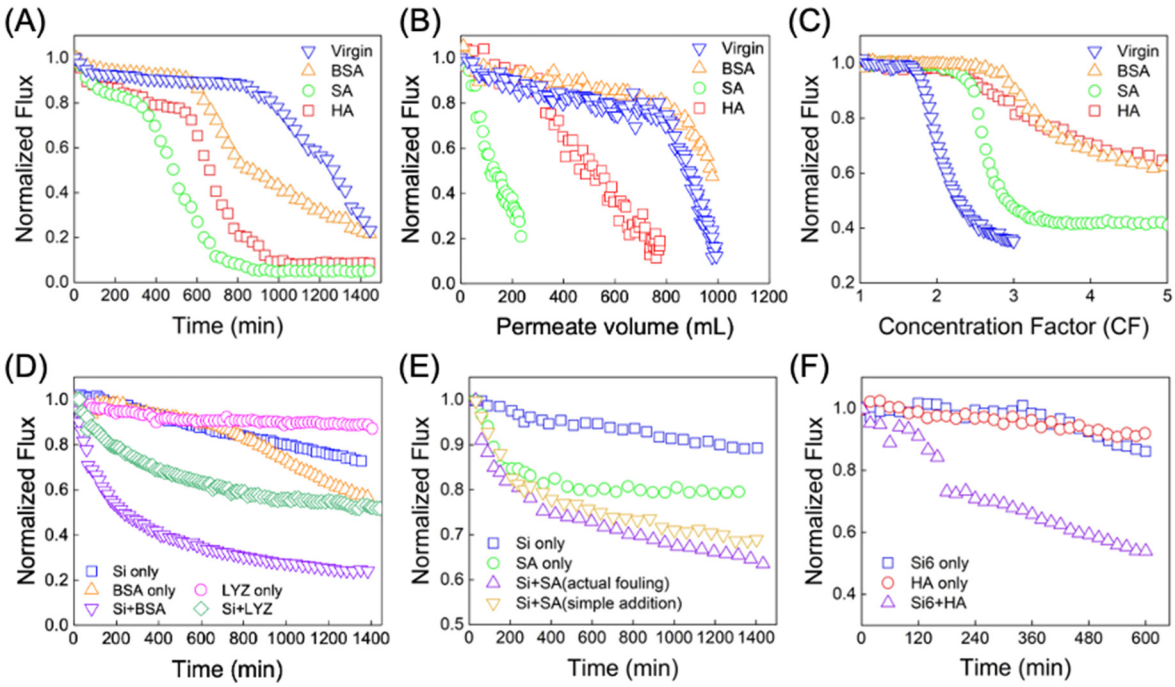

Figure 1. Membrane performance under the combination of mineral scaling and organic fouling. (A) Gypsum scaling on membranes fouled by organic foulants in nanofiltration. (B) Gypsum scaling on membranes fouled by organic foulants in forward osmosis. (C) Gypsum scaling in membrane distillation with the presence of different organic foulants. (D) Silica scaling in reverse osmosis (RO) with the presence of protein bovine serum albumin and lysozyme. (E) Silica scaling in RO with the presence of alginate. (F) Silica scaling in RO with the presence of humic acid. The figures are adapted with permission from ref 50 (A, copyright 2016 Elsevier), ref 53 (B, copyright 2014 Elsevier), ref 55 (C, copyright 2021 Elsevier), ref 30 (D, copyright 2018 American Chemical Society), ref 67 (E, copyright 2020 Elsevier), and ref 31 (F, copyright 2021 Elsevier). The data are extracted from those figures and replotted. Si = silica; BSA = bovine serum albumin; LYZ = lysozyme; SA = sodium alginate; HA = humic acid.

in seawater, groundwater, and wastewater,[13−15] organic fouling is a prevalent issue that has plagued membrane desalination for decades.[12,16−20] Recently, mineral scaling (i.e., inorganic fouling) has attracted increasing attention.[21,22] Mineral scaling occurs when the concentration of solutes exceeds their solubility limit and sparingly soluble minerals subsequently form or deposit on the membrane surface.[21] Mineral scaling is a particularly knotty issue during inland desalination of brackish water, where high concentrations of precursors for various mineral scales (e.g., gypsum, calcite, and silica) are present.[23,24]

Although previous studies have examined the impact of fouling and scaling on membrane performance as well as the underlying mechanisms, organic foulants and inorganic scalants commonly coexist in feedwaters of membrane desalination, potentially imposing a combined effect on membrane performance. For example, both organic fouling and mineral scaling occur in the RO desalination of brackish water in full-scale inland desalination plants.[25,26] Also, fouling and scaling have been simultaneously observed and contributed to the water flux decline in membrane treatment of municipal wastewater[27] and industrial wastewater from the coal chemical industry.[28] Therefore, practical membrane desalination rarely faces the problem of individual fouling or scaling. Instead, membranes are exposed to a mixture of foulants and scalants, which interact with the membrane surface and constrain membrane performance.

Recently, researchers have started to investigate combined fouling and scaling as well as the foulant−scalant interactions. The presence of organic foulants has been shown to regulate homogeneous nucleation of mineral formation by altering the free energy barrier and/or mineral particle aggregation.[29−31] When a layer of organic foulants forms on the membrane surface, the thermodynamics of heterogeneous mineral nucleation or the deposition kinetics of mineral scales could be potentially changed.[32,33] Despite the importance of understanding the coupling of organic fouling and mineral scaling in membrane desalination, the existing literature has only seen review articles that exclusively focus on individual fouling or scaling (i.e., feedwaters contain only organic foulants or mineral scalants).[12,16,21,22,34,35] To the best of our knowledge, there is still a lack of review articles that summarize current knowledge regarding the combined behaviors of organic fouling and mineral scaling, as well as the interactions between foulants and scalants at the water−membrane interface. We acknowledge that combined fouling involving more categories of foulants, including biological and colloidal foulants, is also common in membrane processes. Also, there are studies demonstrating synergistic effects when there is biofouling in the presence of organic foulants[36,37] and some studies indicating a similar effect with combined mineral scaling and biofouling.[38,39] The additivity of combined fouling is dependent on the specific foulants present and the interactions between different types of foulants and membranes. Here, we focus on combined organic fouling and mineral scaling, two common types of fouling in membrane desalination and water treatment.

In this Critical Review, we first describe the impacts of combined fouling and scaling on the performance of membrane desalination (the terms "fouling and foulants" and

https://doi.org/10.1021/acs.est.3c00414
Environ. Sci. Technol. 2023, 57, 7129−7149

"scaling and scalants" are associated with *organic* fouling and *inorganic* scaling hereafter, respectively), particularly focusing on how the coexistence of organic foulants might alter the scaling behaviors of minerals formed *via* both crystallization and polymerization. We then review the state-of-the-art experimental and simulation techniques used to characterize molecular interactions between organics and minerals. Such characterizations reveal the thermodynamics, kinetics, and morphologies of mineral nucleation and growth in the presence of organic substances, playing an essential role in revealing the mechanisms underlying the foulant−scalant interactions. Further, we summarize the current efforts of mitigating combined fouling and scaling *via* membrane materials development and pretreatment. Finally, we propose and discuss future research needs that will help deepen our understanding and design appropriate control approaches associated with membrane desalination facing a combination of organic fouling and mineral scaling.

2. PRESENCE OF ORGANIC FOULANTS ALTERS THE BEHAVIORS OF MINERAL SCALING IN MEMBRANE DESALINATION

2.1. Minerals Formed *via* Crystallization. A variety of mineral scales can be formed *via* crystallization during desalination, such as gypsum ($CaSO_4{\cdot}2H_2O$), calcite ($CaCO_3$), barium sulfate ($BaSO_4$), and calcium phosphate ($Ca_3(PO_4)_2$).[40−42] Among these potential scales, gypsum and calcite are considered to be the most common scales due to the relatively high concentrations of scale precursors in natural waters and wastewater.[43−46] For example, gypsum scaling occurs through crystallization by the reaction of abundant Ca^{2+} and SO_4^{2-} in feedwaters.[47,48] Such crystal-forming reactions can be affected by not only operating conditions but also the feedwater composition, and several studies have demonstrated how organic foulants alter mineral crystallization in different membrane desalination processes. Comparing to mineral scaling, organic fouling has been reported as the major type of fouling that occurs first.[25,49] Consequently, a few studies have investigated the impacts of a pregenerated organic foulant layer on mineral scaling. In such cases, any alteration of membrane scaling extent (e.g., an increase degree of water flux decline) is ascribed to the presence of foulant layer. However, in real-world desalination, membranes are expected to face feedwater containing both mineral scalants and organic foulants simultaneously. Also, mineral nucleation can occur both in the bulk solution and on the membrane surface.[21] As a result, it is also important to investigate combined fouling and scaling when organic foulants coexist with mineral scalants in the feedwater from the beginning. Existing studies on both scenarios are reviewed in this section.

Wang et al.[50] performed a study on the effects of predeposited organic foulant layers on gypsum scaling behavior in NF desalination. As shown in Figure 1A, the membranes fouled by organic foulants experienced more severe flux declines than the virgin membrane, most likely because organic molecules acted as templates for crystallization and led to faster surface crystallization. This synergistic effect was also attributed to the binding of carboxyl groups of the organic foulants to Ca^{2+} ions, promoting organic−Ca^{2+} interactions in the order of SA > HA > BSA (carboxylic acidities: 3.5 > 3.4 > 1 mequiv g^{-1}, respectively).[51] As seen in Figure 1A, the degree and rate of flux decline were consistent with the order of carboxylic acidity. Despite its lowest carboxylic acidity, BSA-fouled membranes still had an induction period shorter than the virgin membrane due to rapid nucleation caused by cake-enhanced concentration polarization.[52] Similar phenomena were observed in the FO process (Figure 1B), where the water fluxes of HA- and SA-fouled membranes decreased faster than the virgin membrane due to high densities of carboxyl groups of HA and SA molecules.[53] Unlike what was observed for NF (Figure 1A), the deposition of a BSA layer slightly mitigated gypsum scaling in the FO process. It was suggested that the heart-shaped structure of BSA at neutral pH could prevent the adsorption of calcium ions by steric effect and thus hinder interactions between BSA and Ca^{2+}.[53] Further, the effect of concentration polarization was proven by Benecke et al.,[54] who performed both static (in beakers) and dynamic (in a cross-flow RO system) experiments with gypsum-supersaturated feed solutions containing organic foulants (SA, HA, or BSA). The results of static experiments showed that bulk crystallization of gypsum was significantly retarded by organic foulants, especially in the presence of SA and HA. During dynamic experiments, however, foulant-induced concentration polarization provoked severe surface crystallization and worsened the overall severity of membrane scaling.

Furthermore, a mitigating effect of organic foulants on crystallization-induced membrane scaling was observed in MD, a hybrid thermal-membrane process. For example, Yan et al.[55] performed MD experiments by adding organic foulants (e.g., SA, HA, or BSA) and scalants together in the feed solutions. The authors demonstrated that all the foulants delayed and slowed water flux decline (Figure 1C), likely because the adsorption of foulants onto membrane surface obstructs gypsum crystallization.[55] Moreover, Wang et al.[29] added various concentrations of HA to gypsum-supersaturated feedwaters for combined fouling and scaling experiments using direct contact MD, where the addition of HA mitigated gypsum scaling and enhanced water recovery. The authors explained that a HA foulant layer on the membrane surface enhanced the free energy barrier to gypsum nucleation.[29] Such an explanation is supported by Curcio et al.,[56] who showed that HA mitigated calcite scaling during MD by increasing the free energy barrier for calcium carbonate nucleation. We note that the effects of organic foulants on the behaviors of crystallization-induced scaling vary between MD and other membrane processes (e.g., Figure 1A,B vs Figure 1C), which could originate from the differences in membrane materials (microporous membranes for MD vs "non-porous" polyamide membranes for RO, NF, and FO[10,12,57]) and/or feedwater composition (the feedwater salinity of RO and NF is lower than that of MD where mineral crystallization in the bulk solution is more prone to occur). Indeed, different behaviors of individual fouling/scaling among different membrane processes have been reported in the literature.[58,59] Comparative studies, which render the behaviors of combined fouling and scaling comparable under different conditions, are needed to connect the roles of organic foulants in regulating the thermodynamics and kinetics of mineral scaling with both membrane and feedwater properties for various membrane technologies.

2.2. Minerals Formed *via* Polymerization. Unlike crystalline scales like calcite and gypsum, silica is unique due to its amorphous structure.[60] Dissolved silica, also known as free silica, mainly consists of monomeric silicic acids, which form colloidal silica by a polymerization reaction.[61,62] The formation of silica scale on membrane surfaces has been shown

https://doi.org/10.1021/acs.est.3c00414
Environ. Sci. Technol. 2023, 57, 7129−7149

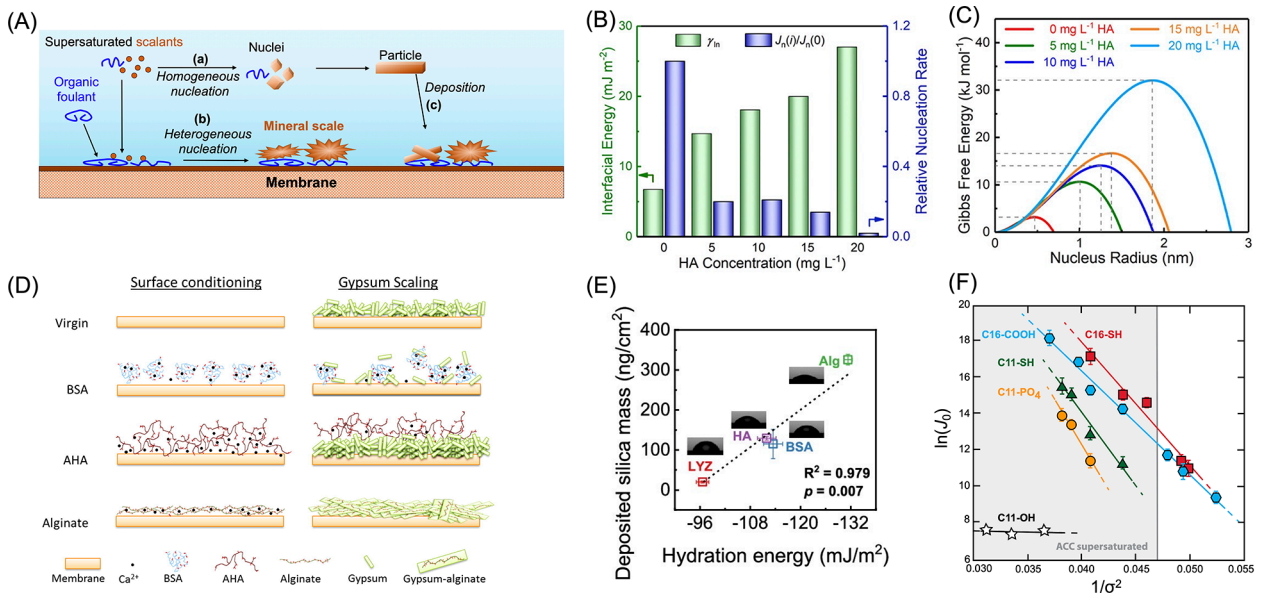

Figure 2. Illustration of how deposited organic foulant layers impact mineral scale formation. (A) Potential mechanisms by which organic foulants impact the nucleation and growth of mineral scales in membrane desalination: (a) regulating homogeneous nucleation by intervening scalant−scalant interactions, (b) altering the free energy barrier to heterogeneous nucleation, and (c) changing the deposition kinetics of scale particles formed in the bulk solution. (B) Effect of humic acid (HA) concentration on gypsum−water interfacial energy and the nucleation rate of gypsum in the bulk solution. (C) Effect of HA concentration on the free energy barrier to gypsum nucleation in the bulk solution. (D) Mechanisms for gypsum scaling on virgin and organic foulant-conditioned forward osmosis membrane. (E) Effect of organic foulant coatings on the formation of silica scale on a quartz crystal microbalance with dissipation (QCM-D) sensor. The deposited silica mass is correlated to the hydrophilicity of the organic foulant-coated surfaces. (F) Measured nucleation rate of calcite on self-assembled monolayer surfaces with different terminating functional groups. Figures B−F are adapted with permission from ref 29 (B and C, copyright 2022 American Chemical Society), ref 53 (D, copyright 2014 Elsevier), ref 33 (E, copyright 2021 American Chemical Society), and ref 80 (F, copyright 2014 United States National Academy of Sciences).

to cause dramatic and usually irreversible decline of water flux during membrane desalination.[63,64] So far, silicic acids have been found to interact with organic molecules including proteins, peptides, and amino acids,[65,66] which could influence the thermodynamics, kinetics, and structure of silica formed by polymerization. The impact of organic matter on the behaviors of silica scaling in desalination process has been explored by several studies.

Quay et al.[30] investigated the combined effect of silica scaling and protein fouling in RO desalination by utilizing two proteins possessing opposite charge at near neutral pH, namely, BSA (negatively charged) and lysozyme (positively charged). The water flux dropped notably faster when protein and silica coexisted than when silica or each protein was present alone in the feed solution (Figure 1D). The underlying mechanisms of such phenomena are different between BSA and lysozyme. The synergistic effect of silica scaling and BSA fouling is ascribed to the formation of silica-BSA aggregates, whereas lysozyme accelerates the polymerization of silicic acid *via* electrostatic attraction between lysozyme and negatively charged silica species.[30]

A similar synergistic effect of silica scaling and SA fouling was reported in RO by Wang et al.[67] As shown in Figure 1E, the water flux decrease caused by combined silica scaling and SA fouling was faster than the sum of water flux decline due to silica scaling and SA fouling individually. The authors suggest that the binding of silica with alginate occurs at carboxyl and hydroxyl groups of alginate molecules *via* noncovalent interaction such as hydrogen bonding and van der Waals interaction.[67] However, contrasting results were reported in a study by Higgin et al.,[68] where the presence of SA reduced silica scaling. To explain the mechanism, the authors pointed to a study by Mavredaki et al.,[69] who showed that carboxyl groups could facilitate the dissolution of amorphous silica. Such a finding, however, was based on synthetic scale inhibitors[69] and has not been proven for the interactions of SA with silica.

The inconsistent findings regarding the effect of SA on silica scaling suggest that our knowledge of combined silica scaling and organic fouling is far from complete, calling for future studies that investigate the silica−organic interactions and their impacts on membrane performance systematically. One factor that potentially alters the effects of organic foulants on silica scaling is the relative concentration of silica to organic foulants. For example, Li et al.[31] studied the effect of HA on silica scaling behavior in the RO process under different silica concentrations (0−10 mM). The synergistic effect of silica scaling and HA fouling was observed at a critical concentration of silica at 6 mM (Figure 1F) but not at lower silica concentrations. The authors explained that, at low concentrations (below 6 mM), silica adsorbed by HA (probably due to the interactions between silica and carboxyl groups of HA molecules) neither altered the morphology of HA nor induced silica aggregation. In contrast, the adsorption sites of HA were saturated when the concentration of silica reached 6 mM. Consequently, self-aggregation of silica and the formation of silica-HA aggregates with larger sizes occurred, thereby facilitating the decrease of water flux.[31]

Compared with membrane scaling caused by mineral crystallization, silica scaling combined with organic fouling has been less studied in desalination processes other than RO (e.g., FO and MD). It is worth mentioning that several studies involving both silica and organic foulants in FO or MD used silica particles (i.e., colloidal fouling) but not silicic acids (i.e.,

https://doi.org/10.1021/acs.est.3c00414
Environ. Sci. Technol. 2023, 57, 7129−7149

silica scaling) in the feed solutions.[70−72] Considering the fundamental difference between silica scaling and colloidal fouling, such studies reveal only the effects of organic foulants on silica particle deposition but not the interactions between organic molecules and silicic acid as well as the subsequent influences on silica scale formation *via* polymerization.

3. MECHANISMS OF MINERAL−ORGANIC INTERACTIONS

3.1. Molecular Interactions of Organic Foulants with Mineral Scalants. In a combined fouling−scaling scenario, organic foulants can play multiple roles in regulating mineral scaling (Figure 2A): (a) regulating homogeneous nucleation by intervening scalant−scalant interactions, (b) altering the free energy barrier to heterogeneous nucleation, and (c) changing the deposition kinetics of scale particles formed in the bulk solution. These effects contribute to the distinct membrane behaviors under combined fouling and scaling as compared with those under individual fouling or scaling, as described in Section 2.

The nucleation and crystallization of gypsum and calcite scales can be disrupted by the presence of organic foulants. Notably, organic foulants such as SA and HA, which have abundant carboxyl groups, are capable of binding with Ca^{2+} and blocking the active sites for the formation and growth of gypsum crystals.[73] HA also suppresses the nucleation of calcite, as reflected by an increase of the induction time in the presence of HA.[56] Such mechanisms are akin to the role of carboxyl-containing antiscalants, such as poly(acrylic acid), in inhibiting gypsum crystallization.[48,74]

As discussed above, silica scale is different from gypsum or calcite scale, as it is amorphous and forms *via* the polymerization of silicic acid. Under neutral pH, monomeric orthosilicic acid ($Si(OH)_4$, $pK_a \sim 9.8$[75]) is predominantly (>99%) in the protonated, neutral form and behaves as a hydrogen bond donor. The oligomer, polymers, and small particles of silica have relatively lower pK_a values[75] and thus carry more negative charge at neutral pH. These silica species can bind with organic foulants *via* a collection of intermolecular forces to form aggregates. It was proposed that BSA can bind with silica *via* hydrogen bonding as well as electrostatic attraction between the positively charged residues and negatively charged silica species.[30,66] These interactions drive the formation of BSA-silica precipitates, which exacerbated water flux decline of RO membranes.[30] Likewise, silica can form hydrogen bonding with the oxygen-containing functional groups (e.g., hydroxyl, carboxyl, and carbonyl groups) of HA, leading to the formation of HA−silica aggregates and a severe decrease in water flux of membrane desalination.[31]

It is worth noting that the interactions between organic foulants and inorganic scalants often depend on their stoichiometry. As discussed above, the synergistic effect of HA fouling and silica scaling only occurred when silica concentration exceeded a critical point.[31] Given the molecular complexity and heterogeneity of organic foulants in various feedwaters of desalination, characterization of the functional groups on organic macromolecules that favorably interact with inorganic scalant species will be instrumental for guiding feedwater pretreatment and other fouling-prevention interventions. For example, various spectroscopic techniques have been employed to characterize the functional groups and metal binding affinities of natural organic matter both qualitatively and quantitatively; interested readers are referred to the literature on this topic.[76,77]

3.2. Organic Foulants Regulate Nucleation of Minerals in the Bulk Solution. As shown in Figure 2A, one important mechanism by which organic foulants regulate mineral scaling is changing the thermodynamics and kinetics of mineral nucleation, crystallization, and/or polymerization in the bulk solution. As a result, the mineral particles formed in the bulk solution, which subsequently deposit onto the membrane surface, have altered particle size, morphology, and/or crystalline structure when organic foulants are present in the feedwater. To elucidate the effects of organic foulants on nucleation and formation of minerals in the bulk solution, we start from introducing the classical nucleation theory (CNT) that describes key parameters that might be affected by foulant−scalant interactions.

The thermodynamic driving force for mineral nucleation and precipitation is manifested by the degree of solution supersaturation σ:

$$\sigma = \ln\left(\frac{\mathrm{IAP}}{K_{sp}}\right) \tag{1}$$

where IAP is the ion activity product and K_{sp} is the solubility product of the mineral. The steady-state nucleation rate, J_0, is related to σ via:

$$J_0 = A\ \exp\left(-\frac{\Delta G^*}{k_B T}\right) \tag{2}$$

where A is the kinetic prefactor that depends on the rates of ion dehydration, attachment, and detachment,[32] ΔG^* is the free energy barrier to nucleation, k_B is the Boltzmann constant, and T is the absolute temperature. For homogeneous nucleation in the bulk solution, ΔG^* can be calculated by eq 3:[21,32]

$$\Delta G^*_{hom} = \frac{F\Omega^2\gamma_{ln}{}^3}{(k_B T\sigma)^2} \tag{3}$$

where F is the nucleus shape factor and is $= 16\pi/3$ for spherical nuclei; Ω is the molecular volume of mineral, γ_{ln} is the free energy of the liquid−nucleus interface. From eqs 2 and 3, one can see that organic macromolecules could regulate the nucleation rate by either changing the kinetic prefactor A or changing the free energy barrier ΔG^* through altering the liquid−nucleus interfacial energy γ_{ln}.

Cao et al.[73] reported that Suwannee River humic acid (SRHA) suppressed gypsum crystallization in the bulk solution. This inhibitory effect was suggested to be caused by the adsorption of SRHA to the gypsum surface, driven by the favorable interaction between carboxyl groups of SRHA and calcium ions. The adsorbed SRHA molecules can also suppress gypsum crystallization by blocking the active growth sites and distorting the crystal morphology.[73] In a study of combined fouling and scaling in MD, Wang et al.[29] observed a similar inhibitory effect of HA on the nucleation and crystallization of gypsum crystals. The authors measured the nucleation rate of gypsum in the bulk solution and observed that increasing HA concentration from 0 to 20 mg/L resulted in a gradual decrease in gypsum nucleation rate (Figure 2B). Through analyses based on the CNT, they found that the presence of HA increased the interfacial free energy (γ_{ln} in eq 3) between a gypsum nucleus and the surrounding solution

https://doi.org/10.1021/acs.est.3c00414
Environ. Sci. Technol. 2023, 57, 7129−7149

(Figure 2B), leading to an increase in the free energy barrier ΔG^* and the critical radius of nuclei (Figure 2C). However, it is unclear whether HA alters the dehydration and association rate of precursor ions (as represented by A in eq 3) due to the small time and length scale of the nucleation process, calling for more mechanistic insights offered by molecular simulations (see Section 4.3).

For silica nucleation that takes place *via* the polymerization of silicic acid monomers, Dove et al.[78] reported that the rate of silica polymerization was enhanced by the presence of small organic molecules such as citric acid and amino acids. Further theoretical analysis in this study revealed that this promoting effect was not of thermodynamic origin, because these organic acids did not alter the free energy of the silica−water interface (γ_{ln} in eq 3). Rather, the organic acids indeed promote silica polymerization via reduction of the kinetic barrier (A in eq 2). It was proposed that the organic acids play several roles in silica polymerization:[78] the deprotonated amino groups (Lewis base) facilitate silica condensation *via* acid−base interaction with the protonated silicic acid; electrostatic interaction and hydrogen bonding between the organic acids and silanol groups of silicic acid also promote silica polymerization. Further, Coradin et al.[65] suggest that the presence of protein lysozyme, which is positively charged at neutral pH, induces silica polymerization *via* electrostatic interactions of the protein with silica precursors, whereas BSA tends to form protein-silica aggregates when coexisting with silica species. Such results are consistent with the synergistically enhanced water flux decline of RO desalination when silica and protein were both present in the feedwater as reported by Quay et al.[30] However, contrasting results were also reported in the literature. For example, Qi et al.[33] recently studied the polymerization kinetics of silica in the presence of 20 mg/L HA, BSA, lysozyme, and SA by monitoring the concentration of molybdate reactive silica (dominantly mono- and disilicic acid[79]) over time. The authors observed no detectable impact of these organics on the bulk polymerization rate of silica. These inconsistent findings suggest that the mechanisms by which organic matter regulates silica polymerization are still poorly understood at the fundamental level and need further investigations.

3.3. Organic Foulants Regulate Surface-Mediated Mineral−Membrane Interactions. Surface-adsorbed organic foulants can regulate mineral scaling by affecting heterogeneous nucleation of minerals and/or the deposition kinetics of mineral particles formed in bulk nucleation (Figure 2A). The deposition of an organic layer on the membrane surface changes the mineral−membrane interactions as well as the subsequent formation of mineral scales and membrane scaling behaviors.[32,33,53,80]

Using direct observation combined with water flux measurement, Liu et al.[53] showed that HA- and SA-conditioning layers accelerated water flux decline in FO and increased the size of gypsum precipitates on the membrane surface; in comparison, BSA conditioning alleviated water flux decline slightly and suppressed gypsum crystal formation (Figure 1C). Further investigations using quartz crystal microbalance with dissipation monitoring (QCM-D) revealed that Ca^{2+} ions were adsorbed favorably on HA- and SA-conditioning layers enriched with carboxyl groups, providing active sites for Ca^{2+} adsorption and the subsequent gypsum nucleation. As a result, a dense gypsum scaling layer was formed on HA- and SA-conditioned membranes. In contrast, BSA contains fewer carboxyl groups and has a heart shape;[81] therefore, the BSA-conditioning layer suppressed gypsum nucleation and crystallization *via* steric effects (see Figure 2D for proposed mechanisms). Similar effects of SA-conditioning layers on gypsum scaling have been also reported in RO systems: at relatively high SA concentration, cake enhanced concentration polarization induced by the SA fouling layer on the membrane hinders back diffusion of scalant ions, enhancing supersaturation at the membrane−water interface and promoting membrane scaling.[54,82]

While most studies focus on the mass and morphology of minerals formed on membranes, there is a sizable knowledge gap in how the crystalline structure of minerals formed on membranes might be altered by the presence of organic foulants. Wang et al.[83] recently studied the role of BSA-conditioning layers in regulating gypsum scaling on RO membrane, with respect to membrane permeability, crystal growth orientation, and crystalline structure of the mineral precipitates. The presence of BSA-conditioning layers slowed the water flux decline caused by gypsum scaling, despite that the mass of precipitated gypsum on BSA-conditioned membrane was twice of that on the virgin membrane. Using grazing incidence wide-angle X-ray scattering (GIWAXS), bassanite, a precursor of gypsum, was found to be present on the BSA-conditioned membrane but not on the virgin membrane. The authors proposed that BSA stabilized bassanite *via* the interaction of carboxyl groups with the Ca^{2+} ions on the (111) crystal facets of bassanite, further disrupting the oriented growth of bassanite to gypsum crystals.

With respect to silica scaling, Qi et al.[33] employed QCM-D and demonstrated that the presence of organic fouling layers impacts silica scale formation *via* both heterogeneous and homogeneous nucleation (Figure 2E). At low supersaturation when heterogeneous nucleation dominated, the mass of silica scale monitored by QCM-D was not correlated with the free energy barrier of heterogeneous nucleation, indicating the importance of kinetic factors rather than thermodynamics in controlling silica nucleation. Rather, the deposited silica mass resulting from heterogeneous nucleation was positively correlated to the hydrophilicity (as manifested by hydration energy) of the macromolecule-coated surface (Figure 2E). At high supersaturation when silica aggregates were formed from nucleation in the bulk solution, the deposited silica mass was related to the strength of macromolecule−silica interaction measured using force spectroscopy.

Organic macromolecules not only impact mineral scaling behaviors in membrane filtration but also underpin the process of biomineralization due to the ubiquitous presence of natural organic matter on environmental surfaces. In particular, the roles of organic matrices in governing calcite and silica nucleation have been extensively studied[32,80,84−87] due to the geochemical significance of these two minerals.[88,89] The knowledge learned from the biomineralization field can be potentially translated to improving the understanding of combined organic fouling and mineral scaling in membrane processes. For example, Dove and co-workers systematically studied how organic substrates with specific functional groups regulate calcite and silica nucleation.[32,80,84,85] For heterogeneous nucleation, the free energy barrier to nucleation, ΔG^*_{het}, can be obtained by eq 4:[32,80]

https://doi.org/10.1021/acs.est.3c00414
Environ. Sci. Technol. 2023, 57, 7129−7149

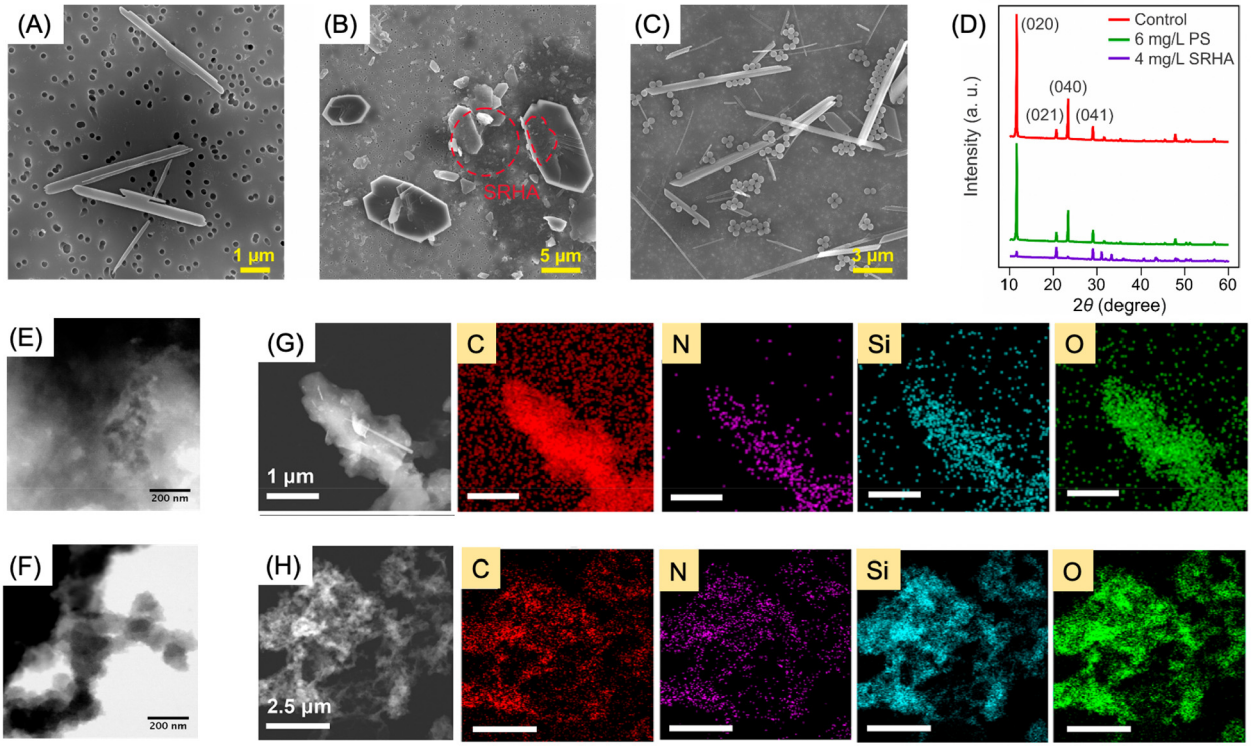

Figure 3. Characterization of foulant-scalant mixtures. (A–C) Morphologies of gypsum crystals formed in the presence of (A) no coexisting foulants, (B) humic acid, and (C) polystyrene latex particles. (D) XRD spectra of these gypsum crystals demonstrate that the presence of humic acid, but not colloidal polymeric particles, distorted gypsum crystal formation. (E–H) Precipitates produced by (E and G) silica and bovine serum albumin or (F and H) silica and lysozyme, as characterized by transmission electron microscopy and energy-dispersive X-ray spectroscopy. Note that the precipitates formed by silica and lysozyme have a stronger signal of Si and a weaker signal of C, indicating silica-BSA precipitates and silica-lysozyme precipitates were distinctly enriched with protein and silica, respectively. The figures are adapted with permission from ref 73 (A–D, copyright 2022 Elsevier) and ref 30 (E–H, copyright 2018 American Chemical Society).

$$\Delta G^*_{het} = \frac{F\Omega^2 {\gamma_{nls}}^3}{(k_B T\sigma)^2} \quad (4)$$

where γ_{nls} is the interfacial free energy of the nucleus–liquid–substrate system, and all other notations are identical with those in eq 3. When organic matter adsorbs on and covers the solid substrate (such as a membrane), the nucleus shape factor F could be changed *via* altering the nucleus–substrate surface free energy. Such alteration is often manifested by incorporating a wetting function (also known as potency factor) $f(\theta)$ where θ is the contact angle between nucleus and substrate.[12,90] In addition, when organic foulants adsorb on the mineral nucleus, the nucleus–liquid interfacial free energy (γ_{ln}) might also be changed, thus altering the intrinsic homogeneous nucleation barrier as shown in eq 3.

To experimentally interrogate the role of organic substrates on mineral surface nucleation, ΔG^*_{het} can be separated into two contributions: solution supersaturation σ and the surface free energy contribution, as represented by B:[32,80]

$$B = \frac{F\Omega^2 {\gamma_{nls}}^3}{k_B^3 T^3} \quad (5)$$

With eqs 4 and 5, eq 2 can be transformed to a linear form:

$$\ln(J_0) = \ln(A) - \frac{B}{\sigma^2} \quad (6)$$

where A is the kinetic prefactor as explained in eq 2. Therefore, the slope of ln (J_0) vs $1/\sigma^2$ indicates the value of B or the substrate-specific surface energy contribution to the barrier of nucleation. Figure 2F presents such a plot for calcite nucleation rates, which were measured on alkanethiol self-assembled monolayers with different head groups (−OH, −COOH, −SH, and $-PO_4$) and chain lengths (C11 and C16).[80] Results show that calcite nucleation rates exhibit a substrate-specific dependence on both headgroup chemistry and chain length. The nucleation rates increase with solution supersaturation (σ), consistent with CNT.[21] On −OH terminated substrates, a low number of calcite crystals were detected, indicating that the −OH group inhibits calcite crystallization. The measured slopes (i.e., B) varied on the other substrates, with the smallest slope observed on the substrate with −COOH headgroup. This indicates that −COOH, an abundant chemistry in natural macromolecules such as humic substances and polysaccharides, could play a key role in promoting calcite nucleation. Further, Wallace et al.[84] investigated the rate of silica nucleation on surfaces modified with organic molecules of different functional groups. The authors reported that the hybrid NH_3^+/COO^- substrates possessed the fastest rate of silica nucleation, and that surface nucleation of silica was more sensitive to kinetic drivers rather than thermodynamic drivers (i.e., the silica nucleation rate was more regulated by A than B in eq 6). These biomineralization studies offered explicit evidence that the presence of organic molecules can alter mineral nucleation due to organic–mineral interactions, parallel to what has been discovered in combined fouling and scaling as discussed above. The fundamental insights gained in these mineralization studies, as well as the associated analytical methods, provide

https://doi.org/10.1021/acs.est.3c00414
Environ. Sci. Technol. 2023, 57, 7129–7149

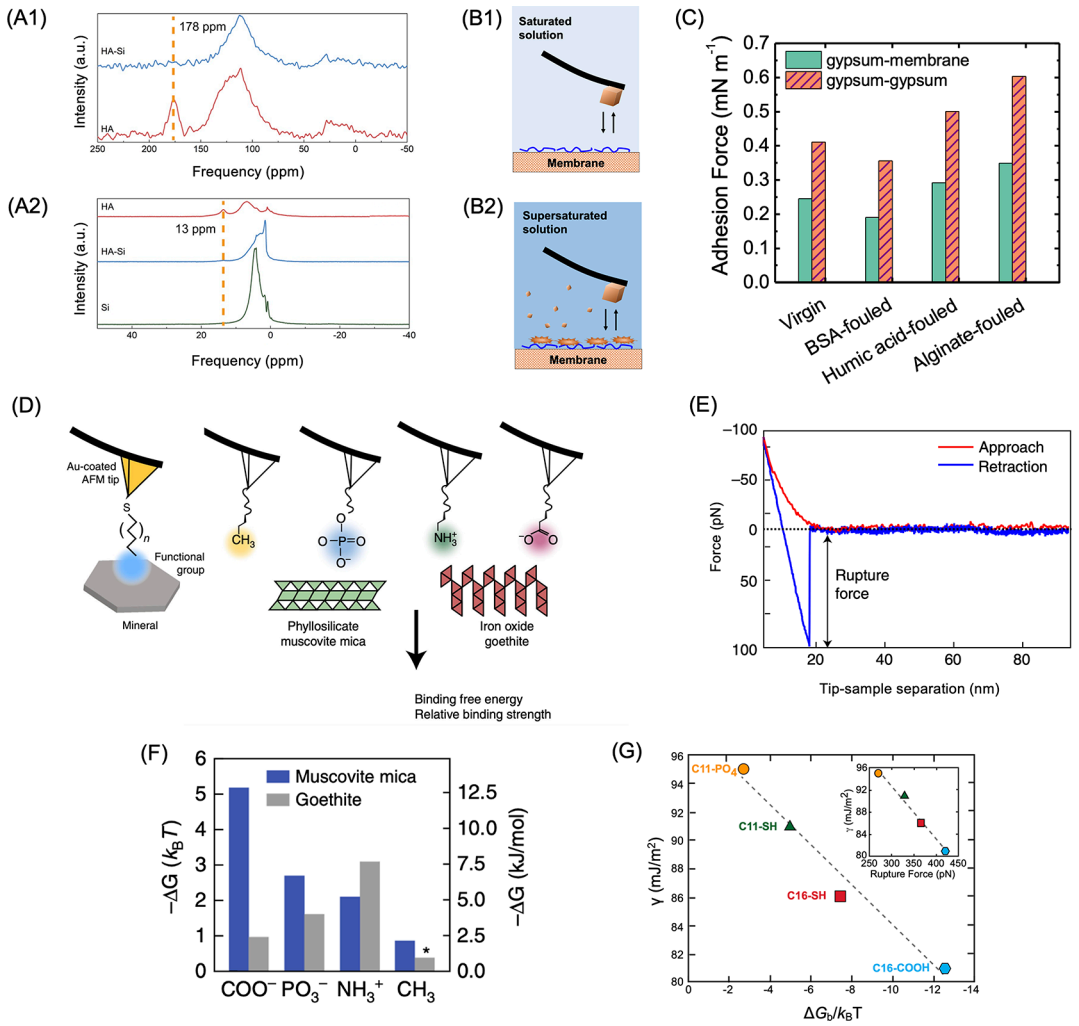

Figure 4. (A) Solid-state nuclear magnetic resonance (NMR) spectra and characteristic peaks for humic acid (HA)−silica mixture, pure HA, and/or pure silica. (A1) ^{13}C solid-state NMR spectra and (A2) ^{1}H solid-state spectra. (B) Schematic showing AFM force measurements between a mineral particle and a fouled membrane surface. (B1) Mineral−membrane interaction measured in a saturated solution. (B2) Mineral−mineral interaction measured in a supersaturated solution, which involves mineral scales formed both on membrane surfaces and in the bulk solution. (C) Measured adhesion force for gypsum−membrane interaction and gypsum−gypsum interaction on virgin and fouled nanofiltration membranes. (D) Schematic showing the measurement of interaction between a mineral surface and an AFM tip functionalized with alkanethiol carrying specific functional groups. (E) Representative force−distance curve showing the rupture force. (F) Binding free energy (ΔG_b) derived from measured rupture forces using dynamic force spectroscopy for an alkanethiol molecule interacting with goethite or mica. Experiments were conducted at pH 6 in 10 mM NaCl. (G) Experimentally derived interfacial energy correlated with binding free energy for an alkanethiol molecule interacting with calcite. Figures A and D−G are adapted with permission from ref 31 (A, copyright 2021 Elsevier), ref 96 (D, E, and F, copyright 2017 Nature Research), and ref 80 (G, copyright 2014 United States National Academy of Sciences). For Figure C, the data were extracted from ref 50 (copyright 2016 Elsevier) and replotted.

valuable avenues to explain and probe organic−mineral interactions in membrane desalination.

4. STATE-OF-THE-ART TECHNIQUES THAT CHARACTERIZE THE INTERACTIONS BETWEEN MINERAL SCALANTS AND ORGANIC FOULANTS

4.1. Structural and Morphological Characterizations of Foulant−Scalant Mixtures. The physicochemical properties of mixtures consisting of organic foulants and mineral scales have been characterized by several techniques. Scanning electron microscopy (SEM) is a widely used technique to examine morphologies of the samples. Thus, the morphological alterations of mineral scales induced by organic foulants are often observed using SEM imaging. For example, Cao et al.[73] utilized SEM to analyze gypsum crystallization in the presence of HA and polystyrene latex particles. While gypsum crystals with the characteristic needle-like morphologies were formed exclusively without foulants (Figure 3A), polygon-like crystals were mainly seen in the presence of HA (Figure 3B). In contrast, polystyrene latex colloidal particles barely altered the morphologies of gypsum crystals (Figure 3C).

As SEM imaging does not provide information on the crystalline structure of the mineral scales, X-ray diffraction (XRD) has been employed to investigate the crystalline features of the formed scales. As shown in Figure 3D, the intensities of characteristic peaks corresponding to the (020) and (040) facets of gypsum were reduced dramatically for gypsum crystals formed with HA, whereas no distinct difference was seen for gypsum coexisting with polystyrene latex particles.[73] This result reveals that HA, but not

https://doi.org/10.1021/acs.est.3c00414
Environ. Sci. Technol. 2023, 57, 7129−7149

polystyrene latex particles, induced change in orientation distribution of the crystalline grains of gypsum crystal, consistent with the morphological changes observed by SEM imaging in Figure 3A,B.

Furthermore, transmission electron microscopy (TEM) is a powerful instrument for morphological and structural characterizations of minerals at a higher resolution than SEM. For instance, Quay et al.[30] characterized precipitates of silica in the presence of two different proteins (i.e., BSA and lysozyme) *via* TEM. The TEM images show that lysozyme-silica precipitates possessed more well-defined particle morphology (Figure 3F) whereas BSA-silica precipitates appeared to be mostly irregular (Figure 3E). The authors further coupled TEM with energy dispersive X-ray spectroscopy (EDX) to provide information on the chemical composition of the precipitates.[30] The EDX elemental mapping showed that BSA- and lysozyme-silica precipitates were both enriched with C, N, Si, and O elements (Figure 3G,H), confirming the coexistence of silica with proteins. Detailed analysis of elemental percentage demonstrated that the lysozyme-silica precipitates were more enriched with Si (Si contents were 2.3−19% and 35.5−42.4% for BSA-silica precipitates and lysozyme-silica precipitates, respectively).[30] This result helped the authors conclude that the BSA−silica interaction generated protein-rich aggregates whereas lysozyme−silica interaction facilitated silica polymerization, showing different mechanisms underlying the synergistic effect of silica scaling and organic fouling observed for proteins carrying different surface charge (Figure 1D).

4.2. Experimental Characterization of Interactions between Organic Foulants and Mineral Scalants. Section 4.1 above describes the experimental techniques that characterize structural and morphological features of foulant−scalant mixtures at the macroscale. In this section, we summarize current advancements that achieve experimental characterization of foulant−scalant interactions at the molecular level.

Attenuated total reflectance Fourier transform infrared (ATR-FTIR) spectroscopy is a convenient tool that reveals the formation of chemical bonds during foulant−scalant interactions. Wang et al.[67] employed ATR-FTIR to investigate the silica−SA mixture. The absorption peaks at 1250 cm^{-1} (Si−C bond) and 1040 cm^{-1} (Si−O−C bond) were observed for the silica−SA mixture, which were not seen in the spectra of pure silica or alginate, implying that stable chemical bonds were formed between silica and alginate. Similarly, nuclear magnetic resonance (NMR) has also been used to identify the chemical interactions between foulants and scalants. The chemical characteristics of the silica−HA mixture were investigated *via* solid state NMR by Li et al.[31] In the ^{13}C NMR spectrum, the carboxyl peak at 178 ppm was observed for HA but not detected for the silica−HA mixture (Figure 4A1). In addition, the characteristic peak of carboxyl hydrogen at 13 ppm disappeared in hydrogen NMR spectrum when silica and HA coexisted (Figure 4A2). These changes indicate that silica interacted with carboxyl group of HA molecules, providing mechanistic insight on the synergistic effect of HA fouling and silica scaling shown in Figure 1F. Also, Preari et al.[79] applied NMR to exploring the effects of uncharged polyethylene glycols (PEGs) on stabilizing silicic acid in supersaturated solutions. The authors demonstrated that the ^{1}H NMR signal due to H-bonded $SiOH/H_2O$ shifted from 6 ppm for pure silica to 7 ppm for the silica−PEG mixture, indicating the formation of strong H-bonds between silica and PEG. The same study also showed that the ^{13}C NMR signal was much narrower and shifted significantly for the silica−PEG mixture compared with pristine PEG, providing additional evidence on the formation of chemical bond between silica and PEG.[79]

As another important technique for analyzing the chemistry of mineral−organic mixtures, X-ray photoelectron spectroscopy (XPS) has been used to examine how organic foulants might alter the local chemical environment of mineral scales. By examining the C 1s spectra, Li et al.[31] showed that the carbon composition of the silica−HA mixture existed mainly in the form of C—H, C—O, C═O, and carboxyl groups, which originate from HA. The decrease of intensity for the characteristic peak corresponding to carboxyl group provided further evidence that the interaction sites of HA with Si were the carboxyl groups of HA, consistent with the results of NMR discussed above. Also, Cao et al.[73] showed that the XPS spectra of Ca element for gypsum scale did not shift, thereby proving that the alteration of gypsum morphology induced by HA (Figure 3A,B) was not due to chemical bonding.

Furthermore, AFM has been widely used to elucidate the mechanisms of organic fouling or mineral scaling during membrane desalination. The measured foulant−membrane or mineral−membrane adhesion was shown to correlate with the degree of water flux decline in the initial filtration stage when foulant/mineral−membrane interactions dominate.[64,91−94] For the scenario of combined fouling and scaling, AFM has also shown a great promise in probing the mechanisms by which organic macromolecules influence mineral scaling. The interactions between foulants and mineral scales involve intermolecular and surface forces, and AFM is well-suited to measure these interactions. The measurements can be conducted in solutions that are saturated or supersaturated with respect to the mineral, so that the effect of bulk nucleation on the interaction forces can be investigated.

To understand the effect of organic fouling layers on gypsum scaling during NF, Wang et al.[50] employed AFM to measure the interaction between a gypsum particle and membranes coated by HA, BSA, and alginate. Two experimental conditions were employed: saturated solution ($\sigma = 0$, Figure 4B1), where the solution was in equilibrium with gypsum but no nucleation took place in the bulk solution, and supersaturated solution ($\sigma > 0$, Figure 4B2), where gypsum particles were formed in the bulk solution *via* homogeneous nucleation and further deposited on the membrane surface. A gypsum particle was attached to the AFM probe *via* the cantilever-moving technique,[95] and the interaction between the gypsum particle and the membrane was recorded when the probe was pulled off from the surface. The adhesion force measured by AFM indicates the strength of binding between the gypsum-functionalized probe and the membrane surface in both conditions, allowing for the determination of gypsum−membrane (Figure 4B1) and gypsum−gypsum (Figure 4B2) interactions. For both types of interactions, the measured adhesion forces (Figure 4C) served as a good indicator for the degree of water flux decline of NF when the membrane was preconditioned with the three organic foulants (see Figure 1A).[50] The measured interaction was the strongest on membranes coated by alginate, indicating the key role of Ca^{2+}-carboxyl affinity in promoting gypsum formation.

In addition to exploring the mechanisms of combined fouling and scaling, AFM-enabled force spectroscopy can also provide fundamental insights into the interactions between organic matter and minerals. Notably, dynamic force spectros-

https://doi.org/10.1021/acs.est.3c00414
Environ. Sci. Technol. 2023, 57, 7129−7149

copy has been used to quantify the binding free energy between organic ligands and minerals.[96,97] In dynamic force spectroscopy, a chemically functionalized AFM tip (Figure 4D) is brought in contact with a mineral surface to form a bond and then pulled away from the surface until the bond is broken during which a rupture force is recorded (Figure 4E). The force measurements are conducted at different pulling rates, such that a plot of rupture force versus pulling rate can be obtained. This approach allows probing the bond breaking in near-equilibrium regime (low pulling rate) and a non-equilibrium regime (high pulling rate). By fitting the curve to a multiple bond breaking theory,[98] the free energy of organic-mineral binding (ΔG_b) can be obtained.

Using this technique, the binding free energies between several organic functional groups ($-COO^-$, $-PO_3^-$, $-NH_3^+$, $-CH_3$) and two minerals (negatively charged phyllosilicate muscovite mica and positively charged iron oxide goethite) were quantified (Figure 4F).[96] The results display a trend that organic ligands and minerals with like charge bind more strongly than pairs that are oppositely charged, suggesting the important role of interactions such as hydrophobic and van der Waals interaction, other than electrostatic forces, in organic–mineral binding. In the study by Hamm et al.,[80] the measured calcite–substrate binding free energy ΔG_b was linearly correlated to the interfacial free energy of the crystal–substrate–liquid system (Figure 4G). This study corroborates the conventional view that a good binder is a good nucleator for mineral formation. While dynamic force spectroscopy has mostly been applied in the (geo)chemistry literature to date,[96,97,99,100] we anticipate that this technique can be a valuable tool for unraveling the molecular-level mechanisms of combined fouling and scaling in membrane processes.

4.3. Molecular Simulations and Their Potentials in Exploring Foulant–Scalant Interactions. Although organic fouling has been intensively investigated by molecular simulations,[101−104] there have been much fewer theoretical studies on mineral scaling during membrane desalination. This is because mineral scaling is a multiscale process that involves complex solution chemistry, solute precipitation, and crystal growth. The wide range of spatiotemporal scale makes it particularly challenging to simulate mineral scaling at the molecular level. To the best of our knowledge, there is still a lack of simulation studies that enable modeling of the *entire* nucleation process of mineral scales, let alone the effects of organic foulants on mineral scale formation. However, gaining such a modeling capability is highly desirable, because a unique advantage of molecular simulation is that it provides a molecular level understanding of the key processes that otherwise is extremely challenging to obtain through experiments alone. Such molecular level of understanding is not only crucial for gaining a fundamental understanding of foulant–scalant interactions, but more importantly, is a prerequisite for enabling an advanced designing strategy for regulating combined organic fouling and mineral scaling. To this end, significant progress has been made in the past to elucidate the key enabling factors for understanding these processes. As a result, a large proportion of this section focuses on the state-of-the-art knowledge on molecular simulation of mineral formation itself, which lays a foundation for understanding the potential of simulation in exploring foulant–scalant interactions.

Mineral scaling commonly found in membrane desalination represents two distinct types of activated processes. The nucleation of crystallization-induced scales such as gypsum and calcite is mainly an *entropic* process, as the rate-limiting steps are the diffusion, dehydration, and agglomeration of ions in solutions. As a result, the free energy barrier is largely entropic, similar to the nucleation of gas hydrates.[105] In contrast, polymerization of silicic acid is characterized by a free energy profile that is mainly *enthalpic*, as the key reaction steps include both Si–O–Si bond formation and water removal from the oligomers. Despite the difference, an accurate representation is required to describe the fundamental interactions of solvated ions in aqueous environment. Although an *ab initio* method is in general considered as the most accurate approach, its computational cost prohibits its application in complex and extended systems. Additionally, density functional theory (DFT) has been shown to often yield incorrect predictions of thermodynamic properties in minerals and solutions,[106] and quantum chemistry method is often required to provide benchmark results. Therefore, the development of less-expensive, but accurate force-field is necessary for enabling the spatiotemporal scale for modeling mineral scaling.

For example, many force fields were developed decades ago for accurately reproducing the structure and mechanical properties of calcite, but they were all shown to fail to predict the phase stability and solvation free energy of calcium ions.[106] This issue was addressed by Raiteri et al.,[106] who reparameterized the rigid-molecule model against experimental free energy difference between calcite and aragonite and experimental free energy of hydration for Ca^{2+}. The authors also developed a flexible model shortly after to account for the angular flexibility of carbonate group,[107] and this force field has been widely used to study nucleation of calcium carbonate.[107,108] Both rigid and flexible models treat carbonate anions as a molecular entity where bonds are predefined and preserved. Although this is an accurate description for both bulk phase and nucleation process, these models are unable to describe carbonate reactivity, which can be relevant for crystal growth process.[109] To address this issue, a reactive force field based on ReaxFF approach[110] was developed.[109] Recently, Raiteri et al.[111] also developed a polarizable force field based on AMOEBA model to improve the standard free energy of ion pairing to form $CaCO_3^0$. The new polarizable model was found to improve the description of solvation structure and transferability. For gypsum, both rigid and polarizable models have been developed recently,[112] paving the way for modeling gypsum nucleation. For silica, since the scaling process proceeds with polymerization of silicic acid, a force field that is able to describe bond-forming and bond-breaking is essential for modeling such process. In this regard, reactive force fields were developed and improved[113−115] to model silica–water interface and sol–gel condensation process.[116] These developments enable gaining important insight into the early stage of the scaling process in a *homogeneous* system that consists of only water and constituent ions, as will be discussed below. For desalination processes that include membranes and organic foulants, the structural and chemical complexity of the system makes modeling more challenging. Simple combination rules are commonly adopted in modeling organic–inorganic interactions, but these rules are only approximate in nature and can often lead to large variations even in simple cases such as Ca^{2+} binding to glycine zwitterion.[117] Therefore, more accurate interactions need to be carefully calibrated through fitting high-quality data.

https://doi.org/10.1021/acs.est.3c00414
Environ. Sci. Technol. 2023, 57, 7129−7149

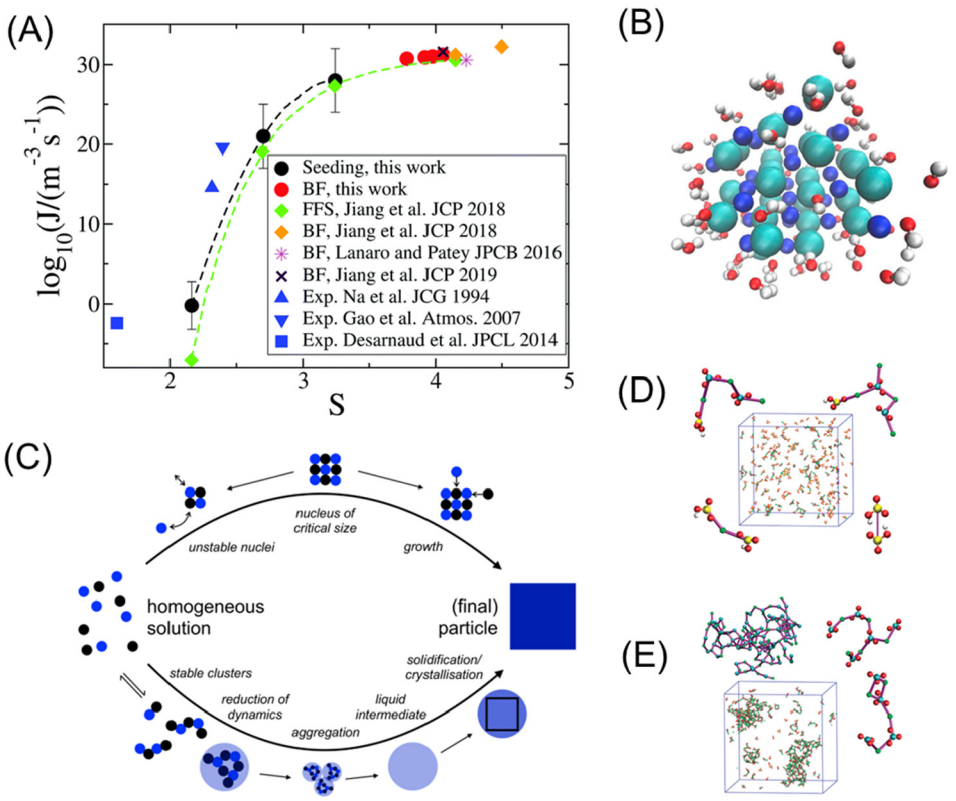

Figure 5. (A) Precipitation of NaCl from solution has been investigated in molecular simulations using advanced sampling methods including forward flux sampling (FFS) and seeding approach combined with CNT at different supersaturations. The homogeneous nucleation rates computed using different methods were found to agree well each other but differ from those from experiments. Note that "this work" in Panel A refers to ref 119 as detailed below. (B) Snapshot of a NaCl nucleus with its first hydration shell obtained from FFS simulation clearly shows a crystalline structure, indicating the precipitation of NaCl under low supersaturation is a classical (one-step) process. (C) Schematic view of classical (top) and nonclassical (bottom) pathways of crystal nucleation from solution. Molecular simulations showed evidence for the existence of stable, liquid-like ionic polymers as prenucleation calcium carbonate clusters that adopt dynamic topology consisting of chains, branches, and rings under (D) low pH and (E) high pH, providing a strong support of nonclassical nucleation mechanism of calcium carbonate. Nevertheless, direct simulation of a true nucleation event from solution has not been achieved for minerals so far, due to extensive spatiotemporal scale and complexity of mineralization process. The figures are adapted with permission from ref 126 (A, copyright 2021 RSC), ref 121 (B, copyright 2018 AIP), ref 184 (C, copyright 2018 MDPI), and ref 108 (D and E, copyright 2011 NPG).

A major challenge in modeling crystal nucleation process is that nucleation is often too "slow" to occur spontaneously in molecular simulation. The slowness is attributed to both the rare-event nature of nucleation and the very limited spatiotemporal scale accessible to molecular simulation. Therefore, standard molecular simulation approaches are usually insufficient for modeling crystal nucleation under experimentally relevant conditions. Interested readers may refer to an excellent review on this topic.[118] Since mineralization proceeds with a solute precipitation process, a unique challenge in molecular simulation of mineralization is the effect of solute depletion. As molecular simulations are typically conducted using a fixed number of atoms/molecules, the formation of a crystal embryo consumes ions in solution, consequently leading to a decrease of chemical potential of solution upon nucleation. This artificial change in driving force for nucleation not only yields a quantitative inaccuracy of crystal nucleation but also may even fundamentally alter the underlying nucleation mechanism. A remedy to this issue is to increase the size of simulation cell so that the change in solution concentration becomes negligible,[119] but this strategy will inevitably lead to a significant increase in computational cost.

Given all these challenges, it is not surprising that no simulation study was reported up to date to model the *entire* nucleation process of mineral scale. In a closely related, but much simpler system, the nucleation of NaCl from supersaturated brine, has been indeed investigated by molecular simulations. These studies provide invaluable insights that may help understand the complex mineralization process. For example, using a large simulation cell, Chakraborty and Patey[120] performed direct molecular dynamics simulation and showed that NaCl nucleation follows a two-step process in that the early stage nucleus is a loosely ordered arrangement of ions containing a significant amount of water, followed by a slow dehydration process as crystal grows. This result contrasted with CNT, which assumes nucleation is a one-step process where the nucleus bears the same structure of the thermodynamically stable phase. However, a later study[121] showed that NaCl was significantly supersaturated in the work of Chakraborty and Patey[120] for the employed force field. Using the forward flux sampling (FFS) method,[122] a rigorous but expensive approach that does not rely on CNT, Jiang et al.[121] showed the nucleation of NaCl under experimentally relevant conditions is better described by CNT. Another advantage of the FFS method is that it allows directly computing nucleation rate, which arguably is the only quantity

https://doi.org/10.1021/acs.est.3c00414
Environ. Sci. Technol. 2023, 57, 7129−7149

that connects experiments and modeling under various conditions. The calculated homogeneous NaCl nucleation rates based on FFS were found to be lower than the experimental rates, which was attributed to the inaccuracy of the force fields in determining the interfacial tension.[121] Indeed, a subtle error in reproducing solid−liquid interfacial free energy can lead to orders of magnitude variation in nucleation rate.[123] Another approach that allows for modeling NaCl nucleation under experiment-relevant conditions is seeding, where a crystalline seed is inserted in liquid to allow its growth (if seed is beyond the critical size) or dissolution (if seed is below the critical size).[124] When combined with CNT, seeding approach can also yield nucleation rate, solid−liquid interfacial free energy, nucleation barrier, and ion-attachment frequency.[119] As nucleation rate is strongly dependent on the critical nucleus size in the seeding approach, errors in determining the optimal local order parameter for computing nucleus size can introduce a substantial uncertainty in rate estimates.[119,125] Importantly, Lamas et al.[126] recently showed an agreement in nucleation rate between FFS and seeding approach can be achieved in a wide range of supersaturation by using a mislabeling criterion in seeding approach. The agreement provides a justification for the applicability of seeding approach in homogeneous NaCl nucleation, which is rather a classical one-step process under low supersaturation, as shown in Figure 5A. In such a case, concentration and structural fluctuations occur simultaneously and coherently so that the formed nucleus bears the crystalline structure, as shown in Figure 5B. Under high supersaturation, the two fluctuations were found to decouple so that the concentration fluctuation first leads to the formation of a dense precursor that does not carry crystalline order, which then transforms into an ordered structure in the second structural fluctuation.[127] The transition from one-step to two-step was found to be driven by phase separation due to a spinodal decomposition at a sufficiently high supersaturation.[127]

The gained insight from NaCl nucleation helps to understand the formation of calcite and gypsum from solution, although the chemical complexity, extended spatiotemporal scale, and sluggish dynamics associated with calcite and gypsum nucleation prevent obtaining a similar level of understanding. So far, no modeling work has reported the *entire* nucleation event in these minerals, but there were extensive theoretical[107,108,117] and experimental[128−131] studies on the structure and dynamics in the prenucleation stage of calcium carbonate. In particular, modeling studies strongly suggest the existence of a prenucleation cluster (PNC) pathway in calcium carbonate,[128] which is fundamentally distinguished from CNT in that it is the change in dynamics rather than the size of cluster that defines the critical transition in liquid−solid phase transformation (Figure 5C). In essence, PNCs, which are highly dynamic clusters of ions that are significantly larger than ion pairs, spontaneously form in solutions,[108] constituting a dynamic equilibrium (Figure 5D,E). Upon the increase of size, the dynamics of large cluster slows down, which forms an interface with solution that can be reduced when large clusters aggregate to form large droplets in a liquid−liquid separation.[129,130] The droplets then undergo dehydration process to form amorphous calcium carbonate (ACC),[132−134] which has been frequently observed experimentally.[132−134] The schematic of the PNC pathway is shown in Figure 5C. Although the PNC pathways provide a better explanation of experiments,[135] it is under debate whether this is the only way for carbonate nucleation, as there were studies that suggest carbonate nucleation can be a classical process.[131,136] In particular, *in situ* characterization showed calcite nucleation on carboxyl-terminated self-assembled monolayers (SAM) can be described well by CNT in that heterogeneous nucleation is enhanced due to the reduced interfacial free energy between carboxyl SAM and calcite.[137] Additionally, a nonclassical nucleation pathway has been also reported for gypsum formation.[138−140]

As mineral nucleation is already complicated in aqueous solution, the role of organic foulants contained in feedwater of desalination in regulating mineralization can become even more elusive. Although early experiments already demonstrated calcite nucleation can be enhanced through controlling the functional groups in SAMs,[137,141] $CaCO_3$ formation can be also suppressed as shown in a recent combined experimental and modeling study incorporating multiwalled carbon nanotube (MWCNT) into polyamide membrane.[142] The authors demonstrated that an interfacial water layer formed on the surface of the carbon-modified membrane surface (using a flat graphitic sheet as a surrogate for MWCNT) hindered the attraction of Ca^{2+} and $CaCO_3$ clusters to the membrane surface. The authors attributed the enhanced antiscaling performance to the induced smooth surface morphology, the decrease of surface charge, and the formation of a rigid interfacial water layer. These results highlight the complex and important roles of inorganic−organic interactions in regulating crystal nucleation. Also, Li et al.[31] used molecular dynamics simulation to reveal that the interactions of silica with HA are through hydrogen bonding and that the carboxyl group of HA is the dominant functional group to bind silica. Such results provide molecular-level support of the NMR results discussed in Section 4.2.

It should be also noted that such interactions are expected to play an equally, if not more, important role in the *growth* of these minerals. In this regard, insight gained in understanding the crystallization of other materials already provides strong indication that inorganic−organic interaction can regulate crystal growth. For example, both molecular modeling[143,144] and experimental[145,146] studies suggest ice-nucleation proteins and antifreeze proteins share very similar structures and functional groups, rending similar ice-binding mechanism, but the difference in their sizes lead to the opposite effects in ice crystallization. Similarly, molecular simulations[147,148] helped elucidate the molecular mechanisms responsible for antiagglomerants used in oil industry that prevent gas hydrate particles from coalescence inside of oil and gas pipelines.[147,148] The similarity between mineral scaling and coalescence of hydrate thus can be enlightening in understanding foulant−scalant coupling in membrane desalination. Although the use of molecular simulations in understanding organic−mineral interactions is still at a very rudimentary state, the progress of molecular modeling in understanding many other materials holds great promise of deepening our mechanistic understanding on combined fouling and scaling in desalination at a molecular level.

5. RESEARCH OPPORTUNITIES OF IMPROVING MEMBRANE PERFORMANCE UNDER COMBINED FOULING AND SCALING

5.1. Surface-Modified Membranes That Possess Resistance to Combined Fouling and Scaling. Developing membranes that are resistant to fouling and/or scaling *via*

https://doi.org/10.1021/acs.est.3c00414
Environ. Sci. Technol. 2023, 57, 7129−7149

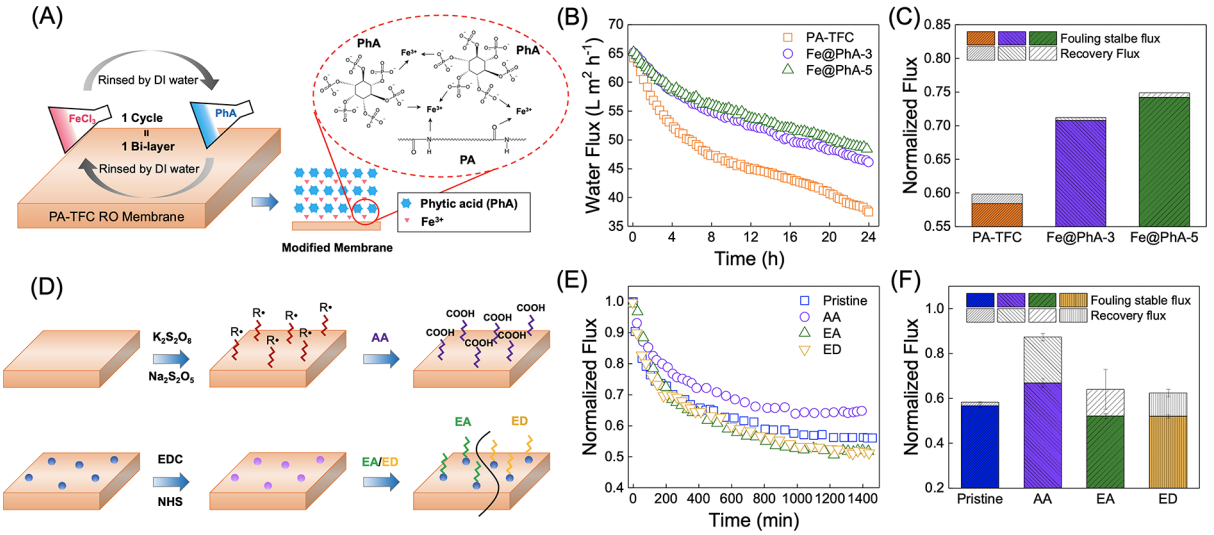

Figure 6. Fabrication and performance of membranes with resistance to combined scaling and fouling. (A) Schematic of the fabrication of polyamide RO membrane modified by multilayered ferric-phytic acid (PhA) complex. (B) Representative water flux decline curves of conventional polyamide membrane and ferric-PhA-modified membrane during combined silica scaling and BSA fouling tests. (C) Normalized water flux after combined scaling−fouling tests and after physical cleaning for membranes in (B). (D) Schematic of the fabrication of polyamide RO membrane modified by acrylic acid (AA), ethylamine (EA), and ethylenediamine (ED). (E) Representative water flux decline curves of conventional polyamide membrane and those modified with AA, EA, and ED during combined silica scaling and alginate fouling. (F) Normalized water flux after combined scaling−fouling tests and after physical cleaning for membranes shown in D and E. The figures are adapted with permission from ref 160 (A−C, copyright 2020 Elsevier) and ref 163 (D and E, copyright 2020 Elsevier). The data are extracted from those figures and replotted.

surface modification is an important strategy to enhance the resilience of membrane desalination. Due to the different mechanisms between organic fouling and mineral scaling, various membrane modification strategies have been employed to enhance membrane resistance against organic fouling[149−153] and mineral scaling.[154−159] Compared with a large number of studies attempting to develop membranes resistant to individual fouling or scaling, only a few studies have been performed to explore the possibility of developing high-performance membranes that have resistance to combined fouling and scaling.

Qi et al.[160] modified the surface of a polyamide RO membrane with multilayered ferric (Fe)-phytic acid (PhA) complex *via* a layer-by-layer (LbL) assembly technique (Figure 6A). The authors demonstrated that the Fe-PhA-modified membranes had slower water flux decline as well as higher flux recovery after membrane cleaning than the pristine polyamide membrane under combined silica scaling and BSA fouling (Figure 6B,C). Such an improvement of membrane performance was attributed to the Fe-PhA multilayer, which rendered the membrane surface more negatively charged, more hydrophilic, and smoother.[160] The enhanced negative surface charge improves membrane resistance against silica scaling *via* repelling ionized silica species,[63] while the improved hydrophilicity and reduced surface roughness reduce the attachment of BSA foulants and BSA−silica aggregates.[160]

The design principle used by Qi et al.[160] above has been also applied to the development of other modified membranes resisting against combined silica scaling and organic fouling. Hao et al.[161] grafted three hydrophilic and negatively charged molecules, including L-*O*-phosphoserine, 3-amino-1-propanesulfonic acid, and alendronate sodium trihydrate, on the RO membrane surface *via* postmodification of interfacial polymerization. When exposed to both organic foulants (HA or BSA) and silica in combined fouling and scaling tests, all the modified membranes exhibited slower flux decline than the pristine membrane. Similarly, Mankol et al.[162] prepared a polyamide RO membrane using 2,5-diaminobenzenesulfonic acid (a sulfonate-containing molecule) as the comonomer with *m*-phenylenediamine in interfacial polymerization. Compared with conventional polyamide membrane, the fabricated membrane surface displayed an enhancement in negative charge, hydrophilicity, and smoothness, showing significantly lower water flux decline during combined silica scaling and BSA fouling experiments. Further, Wang et al.[163] explored the effect of physicochemical property of RO membrane surface on combined silica scaling and SA fouling by grafting molecules possessing different functional groups (i.e., −COOH, $-CH_3$, and $-NH_2$). Acrylic acid (AA) was grafted *via* a redox radical reaction, while ethylamine (EA) and ethylenediamine (ED) were grafted with the assistance of *N*-(3-(dimethylamino)propyl)-*N*-ethylcarbodiimide hydrochloride (EDC) and *N*-hydroxysuccinimide (NHS) (Figure 6D). The AA-modified membrane showed the least extent of water flux decline and the best flux recovery after membrane cleaning, whereas the EA- and ED-modified membranes suffered from slightly facilitated flux decline (Figure 6E,F). The authors demonstrated a strong correlation between membrane surface charge and performance,[163] suggesting that electrostatic repulsion played a key role in the mitigation of silica scaling and SA fouling.

As described above, current studies have developed novel membranes with resistance to combined fouling and scaling by altering membrane surface properties including surface charge, hydrophilicity, and roughness. However, these studies have been dominantly focusing on mitigating silica scaling and organic fouling simultaneously in RO. To the best of our knowledge, there is still a lack of studies that explore the fabrication of high-performance membranes exposed to a combination of organic fouling and crystallization-induced scaling (e.g., gypsum and calcite scaling). Given that the mechanisms between crystallization- and polymerization-

https://doi.org/10.1021/acs.est.3c00414
Environ. Sci. Technol. 2023, 57, 7129−7149

induced scaling are distinct, future research is needed to investigate which membrane surfaces are desired for mitigating combined organic fouling and crystallization-induced scaling. Also, membranes that are resistant to combined fouling and scaling in other membrane processes such as MD and FO have been rarely reported. We noticed that superhydrophobic membranes with slippery property have been demonstrated to reduce both organic fouling and mineral scaling in MD.[85,152,153,156−158,164,165] Superhydrophobic membranes reduce the contact between the feedwater and membrane surface, while creating a slip boundary condition that improves the hydrodynamic behavior.[12,165] Although these mechanisms are potentially applicable to the mitigation of organic fouling, superhydrophobic membranes have not been challenged by feedwaters containing both organic foulants and inorganic scalants at the same time. As a result, corresponding studies should be performed to expand our knowledge on membrane resistance against combined fouling and scaling to membrane processes other than RO, thereby improving the robustness of membranes applied to a wider range of industrial wastewater possessing complex chemical compositions.

5.2. Pretreatment to Remove Foulants and/or Scalants from the Feedwater. Pretreatment of feedwater to remove organic foulants and scale-forming species is commonly used to prolong membrane lifespan.[166,167] The foulants and scalants can be removed individually or simultaneously. From the perspective of combined fouling and scaling, one important criterion for the selection of proper pretreatment strategies is whether the removal of foulants or scalants is beneficial for mitigating membrane performance degradation. When the combined effect of foulants and scalants on membrane performance is synergistic, removing organic matter or scalants potentially eliminates such a synergistic effect and will lead to a lesser decline of water flux. In the case when fouling and scaling have antagonistic effects, however, removing organic foulants alone is undesirable and can cause more severe decay of membrane performance. Regardless of whether synergistic or antagonistic effects exist between fouling and scaling, removing both organic matter and mineral scalant precursors would be beneficial for maintaining the performance of membrane processes over the long-term.

Gypsum, calcite, and magnesium-containing scales are formed from precursors such as calcium and magnesium ions. These divalent hardness ions are more readily removed than silicic acid, which is dominantly neutral at near neutral pH. Apell et al.[168] studied the efficiency of combined ion exchange treatment, which was composed of anion exchange that targeted the removal of dissolved organic carbon (DOC) and cation exchange that removed the hardness ions. The treatment was effective in removing >55% of both DOC and hardness ions. Other studies have also demonstrated the capabilities of ion exchange resins for the removal of precursor ions of mineral scale[169] and organic matter[170] separately. The effectiveness of combined ion exchange was improved in the work by Comstock et al.,[171] who applied magnetically enhanced ion exchange that was able to achieve >75% removal of both DOC and divalent ions. Coagulation-based approaches have also been used to remove organic substances, but they tend to be less effective in removing hardness ions. For example, Hakizimana et al.[172] studied electrocoagulation as pretreatment for RO desalination. They reported that electrocoagulation had the capability of removing >70% of DOC and microorganisms but only negligible removal of the scale precursor ions (≤10%).

There are far fewer studies investigating the performance of pretreatment processes for feedwater containing organic matter and silica, but existing publications on the removal of each constituent may provide potential treatment options. As previously mentioned, electrocoagulation was shown to effectively remove organic matter.[172] Zhang et al.[173] demonstrated a similar electrocoagulation process for 90% removal of silica in brackish water. While each of these studies alone does not provide sufficient evidence that electrocoagulation is effective in simultaneously removing organic matter and silica, they might motivate future studies to investigate its efficiency when both constituents are present. Ho et al.[174] and Subramani et al.[175] both studied various pretreatment options, including coagulation, ultrafiltration, organoclay filters, and MYCLEX cartridges, which showed varied removal of organic matter but low removal (<15%) of silica. A thorough search of the literature failed to find a promising treatment process proven to remove >50% of both organic matter and silica. More research is required to further understand the removal of silica in the presence of organic matter.

Although the literature implies that some pretreatment technologies are effective in removing organic matter and scaling precursors, more investigations that combine pretreatment with desalination processes are needed to probe the mitigating effect of different pretreatment approaches on combined fouling and scaling. Recently, Liu et al.[176] employed UV/Fe(II)/S(IV) (UFS) pretreatment in an attempt to mitigate HA-enhanced gypsum scaling in NF process. The UFS pretreatment generated sulfate radicals that destroyed the structure of carboxyl group, thereby weakening the complexation of Ca^{2+} with HA. As a result, gypsum scaling was mitigated due to the alleviated cake-enhanced osmotic pressure and reduced extent of concentration polarization. Ultimately, the goal of feedwater pretreatment is to reduce the operating costs associated with membrane cleaning and replacement. The fundamental insights gained from studies of combined fouling and scaling, as reviewed in the above sections, have the potential of helping guide the selection of the most effective and economical pretreatment technologies.

6. OUTLOOK OF RESEARCH NEEDS

In this Critical Review, we examined the state-of-the-art knowledge on the behaviors and mechanisms of combined fouling and scaling, experimental characterization and molecular modeling of foulant−scalant interactions, as well as the potential mitigation strategies. Despite these knowledge advances, our understanding of combined fouling and scaling, especially at the molecular level, is far from fully established, warranting future studies on this complex but important topic pertaining to practical scenarios of membrane desalination.

Under the framework of CNT, organic foulants can regulate the rate of mineral nucleation in two primary ways: (1) the adsorption of organics on mineral nuclei in the bulk solution alters the liquid−nucleus interfacial energy and thus changes the free energy barrier to homogeneous nucleation and (2) the coating of membranes by organic foulants changes the rates of heterogeneous nucleation by altering the nucleus shape factor, which can be quantified by incorporating a wetting function $f(\theta)$. However, as discussed above, inconsistent results exist on the effects of organic foulants on mineral scaling in membrane desalination. Hence, more systematic and comparative

https://doi.org/10.1021/acs.est.3c00414
Environ. Sci. Technol. 2023, 57, 7129−7149

investigations are needed to further understand the interplays between organic fouling and mineral scaling as a function of both membrane process and experimental conditions. Revealing the stoichiometric relationship of foulant−scalant coupling, for example, is essential to predicting the behavior of combined fouling and scaling. The gained knowledge will lead to the development of theories and models that can be used to quantify the impacts of organic foulants on the induction time, nucleation rate, and crystal growth of mineral formation. Also, it is important to distinguish the effects of organic foulants on homogeneous and heterogeneous nucleation of minerals formation. Future investigations are needed to decouple the contribution of each nucleation mechanism to combined fouling and scaling. However, as the contributions of homogeneous and heterogeneous nucleation to mineral scaling are still under debate, closing this knowledge gap requires a more complete understanding of mineral scaling itself. Furthermore, although CNT has been commonly used to explain the behaviors of mineral scaling mechanistically, an increasing amount of evidence has been provided on the existence of nonclassical nucleation pathways.[128,140,177] If nonclassical nucleation is more accurate for describing mineral scale formation, the role of foulant−scalant interactions, as well as the mechanisms of combined fouling and scaling, will be revisited. Future studies that attempt to apply nonclassical nucleation pathway to explaining foulant−scalant interactions (i.e., between foulants and PNCs, rather than between foulants and scalant ions) are valuable to developing a more complete theoretical framework for understanding combined fouling and scaling.

We notice that existing literatures dominantly focus on the effects of organic fouling on mineral scaling rather than those of mineral scaling on organic fouling. One challenge to the latter is that some scale precursors, such as Ca^{2+} (i.e., the precursor for gypsum and calcite scaling), have been shown to facilitate organic fouling.[178−180] Even though, it is still beneficial for future investigations to explore the impacts of mineral scaling on the deposition of organic foulants, thereby leading to more comprehensive knowledge on combined fouling and scaling. In addition, more studies are needed to characterize organic foulants and mineral scales attached to membranes taken from real membrane desalination facilities, in order to connect the fundamental knowledge gained from laboratory studies with industrially relevant scenarios. The use of organic substances extracted from real feedwaters of desalination, rather than simplified model foulants dominantly used in existing literatures, can lead to a more accurate understanding of the interactions between organic fouling and mineral scaling in membrane desalination.

Experimental techniques that enable the investigation of the foulant−scalant interactions are essential to elucidate the mechanisms of combined fouling and scaling. Here, we would like to highlight the techniques used in the field of biomineralization, which can be employed to explore the coupling of organic fouling and inorganic scaling. For example, quantifying the rate of mineral nucleation is necessary for understanding the effects of organic foulants on the thermodynamics and kinetics of mineral nucleation. For minerals with relatively fast growth rate such as calcite and gypsum, direct observation with optical microscopy is sufficient.[32,80] However, for minerals with slow nucleation kinetics such as silica, state-of-the-art techniques with higher resolution such as *in situ* fluid cell AFM should be used to measure the number of particles formed at nascent stages immediately following nucleation.[84] By adjusting the residence time of feed solutions in the fluid cell (e.g., shorter or longer than the induction time for homogeneous nucleation), the contributions of homogeneous and heterogeneous nucleation might be decoupled. Also, dynamic force spectroscopy, which has been used to measure mineral-substrate binding free energy, can be a valuable tool to probe the affinity of minerals to membrane substrates, which is associated with nonclassical nucleation (the attachment of PNCs to membrane surfaces) and homogeneous nucleation in the bulk solution (the deposition and attachment of scale particles to membrane surfaces).

Furthermore, we note that current experimental approaches are not able to fully elucidate the mechanisms of combined fouling and scaling. Molecular simulation represents a promising but largely untapped tool that helps us understand foulant−scalant interactions at the molecular level. As analyzed above, despite the current progress in molecular simulation of mineral nucleation, our capabilities of modeling the entire mineral nucleation process, as well as the interactions of organic foulants with inorganic scalants, are very limited. Future studies that develop novel computational methodologies that enable more complete and efficient modeling of mineral nucleation, such as by extending the success in modeling relevant systems such as ice, gas hydrate, and NaCl nucleation to mineral scaling, will be of great value to gain molecular mechanisms of mineral scale formation in the presence of organic foulants.

Lastly, current efforts of improving the performance of membrane desalination need to take the coupling of membrane fouling and scaling into consideration. Antifouling or antiscaling membranes, which have been typically developed to resist against individual fouling or scaling, need to be challenged by feedwaters with both high fouling and high scaling potentials. Such a strategy will provide necessary insights into whether these functional membranes are able to mitigate combined scaling and fouling. Guided by a combination of experimental, theoretical, and computational approaches, we are potentially able to transform and expand the design framework of high-performance membranes from individual fouling/scaling resistance to resistance against combined scaling and fouling. Besides membrane material development, process innovation might also help mitigate combined fouling and scaling. For example, Liu et al.[165,181] showed that applying a pulse flow, which creates regular membrane vibration, was able to reduce both gypsum and silica scaling in MD, probably due to the fluctuation of water−membrane interface that reduces concentration and temperature polarization. This approach of altering the hydrodynamic behavior of membrane processes has the potential to mitigate both mineral scaling and organic fouling, but it needs to be tested with feedwaters containing both scalants and foulants. Further, the use of antiscalants is a common strategy of mitigating mineral scaling.[48,182,183] However, it is still unknown how antiscalants might affect the behaviors of combined fouling and scaling in membrane desalination, as well as whether the presence of organic foulants might alter the efficacy of antiscalants. As a result, future research should be directed to assess the efficiency of antiscalants when mineral scalants and organic foulants coexist in the feedwater and to unveil the effects of antiscalants on foulant−scalant interactions. The above efforts of tackling combined fouling and

https://doi.org/10.1021/acs.est.3c00414
Environ. Sci. Technol. 2023, 57, 7129−7149

scaling are expected to greatly improve the resiliency and efficiency of membrane desalination systems when feedwaters with complex compositions are treated.

AUTHOR INFORMATION

Corresponding Authors

Tiezheng Tong − *Department of Civil and Environmental Engineering, Colorado State University, Fort Collins, Colorado 80523, United States;* orcid.org/0000-0002-9289-3330; Phone: +1(970)491-1913; Email: tiezheng.tong@colostate.edu

Xitong Liu − *Department of Civil and Environmental Engineering, George Washington University, Washington, D.C. 20052, United States;* orcid.org/0000-0002-5197-3422; Phone: +1(202)994-4964; Email: xitongliu@gwu.edu

Tianshu Li − *Department of Civil and Environmental Engineering, George Washington University, Washington, D.C. 20052, United States;* orcid.org/0000-0002-0529-543X; Phone: +1(202)994-3809; Email: tsli@gwu.edu

Authors

Shinyun Park − *Department of Civil and Environmental Engineering, Colorado State University, Fort Collins, Colorado 80523, United States*

Bridget Anger − *Department of Civil and Environmental Engineering, George Washington University, Washington, D.C. 20052, United States*

Complete contact information is available at: https://pubs.acs.org/10.1021/acs.est.3c00414

Notes

The authors declare no competing financial interest.

ACKNOWLEDGMENTS

This material is based upon work supported by the National Science Foundation under Grant No. 2143508 and 2143970.

REFERENCES

(1) Mekonnen, M. M.; Hoekstra, A. Y. Four billion people facing severe water scarcity. *Sci. Adv.* **2016**, *2* (2), e1500323.

(2) Colorado River drought holds long-term problems for 40 million people. https://www.nbcnews.com/meet-the-press/western-u-s-faces-long-term-colorado-river-drought-issues-n1298102 (accessed 2023-03-29).

(3) Wolf, Z. B. More water cuts as the US adjusts to the climate crisis. https://www.cnn.com/2022/08/16/politics/water-cuts-drought-climate-change-what-matters/index.html (accessed 2023-03-29).

(4) China drought causes Yangtze to dry up, sparking shortage of hydropower. https://www.theguardian.com/world/2022/aug/22/china-drought-causes-yangtze-river-to-dry-up-sparking-shortage-of-hydropower (accessed 2023-03-29).

(5) Mauter, M. S.; Zucker, I.; Perreault, F.; Werber, J. R.; Kim, J. H.; Elimelech, M. The role of nanotechnology in tackling global water challenges. *Nature Sustainability* **2018**, *1* (4), 166−175.

(6) Elimelech, M.; Phillip, W. A. The future of seawater desalination: Energy, technology, and the environment. *Science* **2011**, *333* (6043), 712−717.

(7) Shannon, M. A.; Bohn, P. W.; Elimelech, M.; Georgiadis, J. G.; Marinas, B. J.; Mayes, A. M. Science and technology for water purification in the coming decades. *Nature* **2008**, *452* (7185), 301−310.

(8) Werber, J. R.; Osuji, C. O.; Elimelech, M. Materials for next-generation desalination and water purification membranes. *Nat. Rev. Mater.* **2016**, *1* (5), 16018.

(9) Tong, T.; Elimelech, M. The global rise of zero liquid discharge for wastewater management: Drivers, technologies, and future directions. *Environ. Sci. Technol.* **2016**, *50* (13), 6846−6855.

(10) Shaffer, D. L.; Werber, J. R.; Jaramillo, H.; Lin, S.; Elimelech, M. Forward osmosis: Where are we now? *Desalination* **2015**, *356*, 271−284.

(11) Deshmukh, A.; Boo, C.; Karanikola, V.; Lin, S.; Straub, A. P.; Tong, T.; Warsinger, D. M.; Elimelech, M. Membrane distillation at the water-energy nexus: limits, opportunities, and challenges. *Energy Environ. Sci.* **2018**, *11* (5), 1177−1196.

(12) Horseman, T.; Yin, Y.; Christie, K. S. S.; Wang, Z.; Tong, T.; Lin, S. Wetting, Scaling, and Fouling in Membrane Distillation: State-of-the-Art Insights on Fundamental Mechanisms and Mitigation Strategies. *ACS ES&T Engineering* **2021**, *1* (1), 117−140.

(13) Rose, A. L.; Waite, T. D. Effect of dissolved natural organic matter on the kinetics of ferrous iron oxygenation in seawater. *Environ. Sci. Technol.* **2003**, *37* (21), 4877−4886.

(14) Liu, H. M.; Amy, G. Modeling Partitioning and Transport Interactions between Natural Organic-Matter and Polynuclear Aromatic-Hydrocarbons in Groundwater. *Environ. Sci. Technol.* **1993**, *27* (8), 1553−1562.

(15) Amy, G. Fundamental understanding of organic matter fouling of membranes. *Desalination* **2008**, *231* (1−3), 44−51.

(16) Jiang, S. X.; Li, Y. N.; Ladewig, B. P. A review of reverse osmosis membrane fouling and control strategies. *Sci. Total Environ.* **2017**, *595*, 567−583.

(17) Pandey, S. R.; Jegatheesan, V.; Baskaran, K.; Shu, L. Fouling in reverse osmosis (RO) membrane in water recovery from secondary effluent: a review. *Reviews in Environmental Science and Bio-Technology* **2012**, *11* (2), 125−145.

(18) Potts, D. E.; Ahlert, R. C.; Wang, S. S. A Critical-Review of Fouling of Reverse-Osmosis Membranes. *Desalination* **1981**, *36* (3), 235−264.

(19) Ly, Q. V.; Hu, Y.; Li, J.; Cho, J.; Hur, J. Characteristics and influencing factors of organic fouling in forward osmosis operation for wastewater applications: A comprehensive review. *Environ. Int.* **2019**, *129*, 164−184.

(20) Tijing, L. D.; Woo, Y. C.; Choi, J.-S.; Lee, S.; Kim, S.-H.; Shon, H. K. Fouling and its control in membrane distillation—A review. *J. Membr. Sci.* **2015**, *475*, 215−244.

(21) Tong, T. Z.; Wallace, A. F.; Zhao, S.; Wang, Z. Mineral scaling in membrane desalination: Mechanisms, mitigation strategies, and feasibility of scaling-resistant membranes. *J. Membr. Sci.* **2019**, *579*, 52−69.

(22) Rolf, J.; Cao, T.; Huang, X.; Boo, C.; Li, Q.; Elimelech, M. Inorganic Scaling in Membrane Desalination: Models, Mechanisms, and Characterization Methods. *Environ. Sci. Technol.* **2022**, *56* (12), 7484−7511.

(23) Stanton, J. S.; Anning, D. W.; Brown, C. J.; Moore, R. B.; McGuire, V. L.; Qi, S. L.; Harris, A. C.; Dennehy, K. F.; McMahon, P. B.; Degnan, J. R. *Brackish groundwater in the United States*; US Geological Survey, 2017.

(24) Bond, R.; Veerapaneni, S. *Zero Liquid Discharge for Inland Desalination*; Awwa Research Foundation, 2007.

(25) Yang, H. L.; Huang, C.; Pan, J. R. Characteristics of RO foulants in a brackish water desalination plant. *Desalination* **2008**, *220* (1−3), 353−358.

(26) Tran, T.; Bolto, B.; Gray, S.; Hoang, M.; Ostarcevic, E. An autopsy study of a fouled reverse osmosis membrane element used in a brackish water treatment plant. *Water Res.* **2007**, *41* (17), 3915−3923.

(27) Kimura, K.; Okazaki, S.; Ohashi, T.; Watanabe, Y. Importance of the co-presence of silica and organic matter in membrane fouling for RO filtering MBR effluent. *J. Membr. Sci.* **2016**, *501*, 60−67.

(28) Wang, S.; Xiao, K.; Huang, X. Characterizing the roles of organic and inorganic foulants in RO membrane fouling development:

The case of coal chemical wastewater treatment. *Sep. Purif. Technol.* **2019**, *210*, 1008−1016.
(29) Wang, P.; Cheng, W.; Zhang, X.; Liu, Q.; Li, J.; Ma, J.; Zhang, T. Membrane Scaling and Wetting in Membrane Distillation: Mitigation Roles Played by Humic Substances. *Environ. Sci. Technol.* **2022**, *56* (5), 3258−3266.
(30) Quay, A. N.; Tong, T. Z.; Hashmi, S. M.; Zhou, Y.; Zhao, S.; Elimelech, M. Combined Organic Fouling and Inorganic Scaling in Reverse Osmosis: Role of Protein-Silica Interactions. *Environ. Sci. Technol.* **2018**, *52* (16), 9145−9153.
(31) Li, D.; Lin, W.; Shao, R.; Shen, Y.-X.; Zhu, X.; Huang, X. Interaction between humic acid and silica in reverse osmosis membrane fouling process: A spectroscopic and molecular dynamics insight. *Water Res.* **2021**, *206*, 117773.
(32) Giuffre, A. J.; Hamm, L. M.; Han, N.; De Yoreo, J. J.; Dove, P. M. Polysaccharide chemistry regulates kinetics of calcite nucleation through competition of interfacial energies. *Proc. Natl. Acad. Sci. U.S.A.* **2013**, *110* (23), 9261−9266.
(33) Qi, Y.; Tong, T.; Liu, X. Mechanisms of Silica Scale Formation on Organic Macromolecule-Coated Surfaces. *ACS ES&T Water* **2021**, *1* (8), 1826−1836.
(34) Antony, A.; Low, J. H.; Gray, S.; Childress, A. E.; Le-Clech, P.; Leslie, G. Scale formation and control in high pressure membrane water treatment systems: A review. *J. Membr. Sci.* **2011**, *383* (1), 1−16.
(35) Warsinger, D. M.; Swaminathan, J.; Guillen-Burrieza, E.; Arafat, H. A.; Lienhard V, J. H. Scaling and fouling in membrane distillation for desalination applications: A review. *Desalination* **2015**, *356*, 294−313.
(36) Zhao, F.; Xu, K.; Ren, H.; Ding, L.; Geng, J.; Zhang, Y. Combined effects of organic matter and calcium on biofouling of nanofiltration membranes. *J. Membr. Sci.* **2015**, *486*, 177−188.
(37) Zhu, L.-J.; Zhu, L.-P.; Zhao, Y.-F.; Zhu, B.-K.; Xu, Y.-Y. Anti-fouling and anti-bacterial polyethersulfone membranes quaternized from the additive of poly (2-dimethylamino ethyl methacrylate) grafted SiO 2 nanoparticles. *Journal of Materials Chemistry A* **2014**, *2* (37), 15566−15574.
(38) Thompson, J.; Lin, N.; Lyster, E.; Arbel, R.; Knoell, T.; Gilron, J.; Cohen, Y. RO membrane mineral scaling in the presence of a biofilm. *J. Membr. Sci.* **2012**, *415*, 181−191.
(39) Ashfaq, M. Y.; Al-Ghouti, M. A.; Zouari, N. Functionalization of reverse osmosis membrane with graphene oxide and polyacrylic acid to control biofouling and mineral scaling. *Sci. Total Environ.* **2020**, *736*, 139500.
(40) Tzotzi, C.; Pahiadaki, T.; Yiantsios, S.; Karabelas, A.; Andritsos, N. A study of $CaCO_3$ scale formation and inhibition in RO and NF membrane processes. *J. Membr. Sci.* **2007**, *296* (1−2), 171−184.
(41) Cao, Z. Q.; Hu, Y. D.; Zhao, H. Z.; Cao, B.; Zhang, P. Sulfate mineral scaling: From fundamental mechanisms to control strategies. *Water Res.* **2022**, *222*, 118945.
(42) Mangal, M. N.; Salinas-Rodriguez, S. G.; Dusseldorp, J.; Kemperman, A. J. B.; Schippers, J. C.; Kennedy, M. D.; van der Meer, W. G. J. Effectiveness of antiscalants in preventing calcium phosphate scaling in reverse osmosis applications. *J. Membr. Sci.* **2021**, *623*, 119090.
(43) Dydo, P.; Turek, M.; Ciba, J. Scaling analysis of nanofiltration systems fed with saturated calcium sulfate solutions in the presence of carbonate ions. *Desalination* **2003**, *159* (3), 245−251.
(44) Busca, G. Bases and Basic Materials in Industrial and Environmental Chemistry: A Review of Commercial Processes. *Ind. Eng. Chem. Res.* **2009**, *48* (14), 6486−6511.
(45) Le Gouellec, Y. A.; Elimelech, M. Calcium sulfate (gypsum) scaling in nanofiltration of agricultural drainage water. *J. Membr. Sci.* **2002**, *205* (1−2), 279−291.
(46) Le Gouellec, Y. A.; Elimelech, M. Control of calcium sulfate (gypsum) scale in nanofiltration of saline agricultural drainage water. *Environmental Engineering Science* **2002**, *19* (6), 387−397.
(47) Christie, K. S. S.; Yin, Y.; Lin, S.; Tong, T. Distinct Behaviors between Gypsum and Silica Scaling in Membrane Distillation. *Environ. Sci. Technol.* **2020**, *54* (1), 568−576.
(48) Yin, Y. M.; Jeong, N.; Minjarez, R.; Robbins, C. A.; Carlson, K. H.; Tong, T. Z. Contrasting Behaviors between Gypsum and Silica Scaling in the Presence of Antiscalants during Membrane Distillation. *Environ. Sci. Technol.* **2021**, *55* (8), 5335−5346.
(49) Huiting, H.; Kappelhof, J.; Bosklopper, T. G. Operation of NF/RO plants: from reactive to proactive. *Desalination* **2001**, *139* (1−3), 183−189.
(50) Wang, J.; Wang, L.; Miao, R.; Lv, Y.; Wang, X.; Meng, X.; Yang, R.; Zhang, X. Enhanced gypsum scaling by organic fouling layer on nanofiltration membrane: Characteristics and mechanisms. *Water Res.* **2016**, *91*, 203−213.
(51) Mi, B.; Elimelech, M. Chemical and physical aspects of organic fouling of forward osmosis membranes. *J. Membr. Sci.* **2008**, *320* (1−2), 292−302.
(52) Hoek, E. M. V.; Elimelech, M. Cake-enhanced concentration polarization: A new fouling mechanism for salt-rejecting membranes. *Environ. Sci. Technol.* **2003**, *37* (24), 5581−5588.
(53) Liu, Y. L.; Mi, B. X. Effects of organic macromolecular conditioning on gypsum scaling of forward osmosis membranes. *J. Membr. Sci.* **2014**, *450*, 153−161.
(54) Benecke, J.; Rozova, J.; Ernst, M. Anti-scale effects of select organic macromolecules on gypsum bulk and surface crystallization during reverse osmosis desalination. *Sep. Purif. Technol.* **2018**, *198*, 68−78.
(55) Yan, Z. S.; Qu, F. S.; Liang, H.; Yu, H. R.; Pang, H. L.; Rong, H. W.; Fan, G. D.; Van der Bruggen, B. Effect of biopolymers and humic substances on gypsum scaling and membrane wetting during membrane distillation. *J. Membr. Sci.* **2021**, *617*, 118638.
(56) Curcio, E.; Ji, X. S.; Di Profio, G.; Sulaiman, A.; Fontananova, E.; Drioli, E. Membrane distillation operated at high seawater concentration factors: Role of the membrane on $CaCO_3$ scaling in presence of humic acid. *J. Membr. Sci.* **2010**, *346* (2), 263−269.
(57) Zhao, Y.; Tong, T.; Wang, X.; Lin, S.; Reid, E. M.; Chen, Y. Differentiating solutes with precise nanofiltration for next generation environmental separations: a review. *Environ. Sci. Technol.* **2021**, *55* (3), 1359−1376.
(58) Siddiqui, F. A.; She, Q.; Fane, A. G.; Field, R. W. Exploring the differences between forward osmosis and reverse osmosis fouling. *J. Membr. Sci.* **2018**, *565*, 241−253.
(59) Tow, E. W.; Warsinger, D. M.; Trueworthy, A. M.; Swaminathan, J.; Thiel, G. P.; Zubair, S. M.; Myerson, A. S. Comparison of fouling propensity between reverse osmosis, forward osmosis, and membrane distillation. *J. Membr. Sci.* **2018**, *556*, 352−364.
(60) Milne, N. A.; O'Reilly, T.; Sanciolo, P.; Ostarcevic, E.; Beighton, M.; Taylor, K.; Mullett, M.; Tarquin, A. J.; Gray, S. R. Chemistry of silica scale mitigation for RO desalination with particular reference to remote operations. *Water Res.* **2014**, *65*, 107−133.
(61) Iler, R. K. *The Chemistry of Silica: Solubility, Polymerization, Colloid and Surface Properties and Biochemistry of Silica*; John Wiley and Sons, 1979.
(62) Makrides, A. C.; Turner, M.; Slaughter, J. Concensation of silica from supersaturated silicic-acid solutions. *J. Colloid Interface Sci.* **1980**, *73* (2), 345−367.
(63) Tong, T.; Zhao, S.; Boo, C.; Hashmi, S. M.; Elimelech, M. Relating Silica Scaling in Reverse Osmosis to Membrane Surface Properties. *Environ. Sci. Technol.* **2017**, *51* (8), 4396−4406.
(64) Mi, B. X.; Elimelech, M. Silica scaling and scaling reversibility in forward osmosis. *Desalination* **2013**, *312*, 75−81.
(65) Coradin, T.; Coupe, A.; Livage, J. Interactions of bovine serum albumin and lysozyme with sodium silicate solutions. *Colloids and Surfaces B-Biointerfaces* **2003**, *29* (2−3), 189−196.
(66) Coradin, T.; Livage, J. Effect of some amino acids and peptides on silicic acid polymerization. *Colloids and Surfaces B-Biointerfaces* **2001**, *21* (4), 329−336.

https://doi.org/10.1021/acs.est.3c00414
Environ. Sci. Technol. 2023, 57, 7129−7149

(67) Wang, S.; Huang, X.; Elimelech, M. Complexation between dissolved silica and alginate molecules: Implications for reverse osmosis membrane fouling. *J. Membr. Sci.* **2020**, *605*, 118109.
(68) Higgin, R.; Howe, K. J.; Mayer, T. M. Synergistic behavior between silica and alginate: Novel approach for removing silica scale from RO membranes. *Desalination* **2010**, *250* (1), 76−81.
(69) Mavredaki, E.; Neofotistou, E.; Demadis, K. D. Inhibition and dissolution as dual mitigation approaches for colloidal silica fouling and deposition in process water systems: Functional synergies. *Ind. Eng. Chem. Res.* **2005**, *44* (17), 7019−7026.
(70) Motsa, M. M.; Mamba, B. B.; Verliefde, A. R. D. Combined colloidal and organic fouling of FO membranes: The influence of foulant-foulant interactions and ionic strength. *J. Membr. Sci.* **2015**, *493*, 539−548.
(71) Qin, W. L.; Xie, Z. L.; Ng, D.; Ye, Y.; Ji, X. S.; Gray, S.; Zhang, J. H. Comparison of colloidal silica involved fouling behavior in three membrane distillation configurations using PTFE membrane. *Water Res.* **2018**, *130*, 343−352.
(72) Qin, W. L.; Zhang, J. H.; Xie, Z. L.; Ng, D.; Ye, Y.; Gray, S. R.; Xie, M. Synergistic effect of combined colloidal and organic fouling in membrane distillation: Measurements and mechanisms. *Environmental Science-Water Research & Technology* **2017**, *3* (1), 119−127.
(73) Cao, T. C.; Rolf, J.; Wang, Z. X.; Violet, C.; Elimelech, M. Distinct impacts of natural organic matter and colloidal particles on gypsum crystallization. *Water Res.* **2022**, *218*, 118500.
(74) Yin, Y.; Kalam, S.; Livingston, J. L.; Minjarez, R.; Lee, J.; Lin, S.; Tong, T. The use of anti-scalants in gypsum scaling mitigation: Comparison with membrane surface modification and efficiency in combined reverse osmosis and membrane distillation. *J. Membr. Sci.* **2022**, *643*, 120077.
(75) Belton, D. J.; Deschaume, O.; Perry, C. C. An overview of the fundamentals of the chemistry of silica with relevance to biosilicification and technological advances. *Febs Journal* **2012**, *279* (10), 1710−1720.
(76) Chen, J.; Gu, B. H.; LeBoeuf, E. J.; Pan, H. J.; Dai, S. Spectroscopic characterization of the structural and functional properties of natural organic matter fractions. *Chemosphere* **2002**, *48* (1), 59−68.
(77) Chen, W.; Yu, H. Q. Advances in the characterization and monitoring of natural organic matter using spectroscopic approaches. *Water Res.* **2021**, *190*, 116759.
(78) Dove, P. M.; Han, N. Z.; Wallace, A. F. Systematic dependence of kinetic and thermodynamic barriers to homogeneous silica nucleation on NaCl and amino acids. *J. Mater. Res.* **2019**, *34* (3), 442−455.
(79) Preari, M.; Spinde, K.; Lazic, J.; Brunner, E.; Demadis, K. D. Bioinspired Insights into Silicic Acid Stabilization Mechanisms: The Dominant Role of Polyethylene Glycol-Induced Hydrogen Bonding. *J. Am. Chem. Soc.* **2014**, *136* (11), 4236−4244.
(80) Hamm, L. M.; Giuffre, A. J.; Han, N.; Tao, J. H.; Wang, D. B.; De Yoreo, J. J.; Dove, P. M. Reconciling disparate views of template-directed nucleation through measurement of calcite nucleation kinetics and binding energies. *Proc. Natl. Acad. Sci. U.S.A.* **2014**, *111* (4), 1304−1309.
(81) Ferrer, M. L.; Duchowicz, R.; Carrasco, B.; de la Torre, J. G.; Acuna, A. U. The conformation of serum albumin in solution: a combined phosphorescence depolarization-hydrodynamic modeling study. *Biophysical journal* **2001**, *80* (5), 2422−2430.
(82) Karanasiou, A.; Karabelas, A. J.; Mitrouli, S. T. Incipient membrane scaling in the presence of polysaccharides during reverse osmosis desalination in spacer-filled channels. *Desalination* **2021**, *500*, 114821.
(83) Wang, M.; Cao, B.; Hu, Y. D.; Rodrigues, D. F. Mineral Scaling on Reverse Osmosis Membranes: Role of Mass, Orientation, and Crystallinity on Permeability. *Environ. Sci. Technol.* **2021**, *55* (23), 16110−16119.
(84) Wallace, A. F.; DeYoreo, J. J.; Dove, P. M. Kinetics of silica nucleation on carboxyl-and amine-terminated surfaces: insights for biomineralization. *J. Am. Chem. Soc.* **2009**, *131* (14), 5244−5250.
(85) Wallace, A. F.; Dove, P. M. Towards an understanding of biosilicification mechanisms: Nucleation of amorphous silica on organic surfaces. *Geochim. Cosmochim. Acta* **2007**, *71* (15), A1081−A1081.
(86) Cusack, M.; Freer, A. Biomineralization: elemental and organic influence in carbonate systems. *Chem. Rev.* **2008**, *108* (11), 4433−4454.
(87) Mann, S.; Archibald, D. D.; Didymus, J. M.; Douglas, T.; Heywood, B. R.; Meldrum, F. C.; Reeves, N. J. Crystallization at inorganic-organic interfaces: biominerals and biomimetic synthesis. *Science* **1993**, *261* (5126), 1286−1292.
(88) Branson, O.; Bonnin, E. A.; Perea, D. E.; Spero, H. J.; Zhu, Z.; Winters, M.; Hönisch, B.; Russell, A. D.; Fehrenbacher, J. S.; Gagnon, A. C. Nanometer-scale chemistry of a calcite biomineralization template: Implications for skeletal composition and nucleation. *Proc. Natl. Acad. Sci. U. S. A.* **2016**, *113* (46), 12934−12939.
(89) Tobler, D. J.; Benning, L. G. In situ and time resolved nucleation and growth of silica nanoparticles forming under simulated geothermal conditions. *Geochim. Cosmochim. Acta* **2013**, *114*, 156−168.
(90) Wu, W.; Nancollas, G. H. Interfacial Free Energies and Crystallization in Aqueous Media. *J. Colloid Interface Sci.* **1996**, *182* (2), 365−373.
(91) Li, Q. L.; Elimelech, M. Organic fouling and chemical cleaning of nanofiltration membranes: Measurements and mechanisms. *Environ. Sci. Technol.* **2004**, *38* (17), 4683−4693.
(92) Lee, S.; Elimelech, M. Relating organic fouling of reverse osmosis membranes to intermolecular adhesion forces. *Environ. Sci. Technol.* **2006**, *40* (3), 980−987.
(93) Mi, B. X.; Elimelech, M. Gypsum Scaling and Cleaning in Forward Osmosis: Measurements and Mechanisms. *Environ. Sci. Technol.* **2010**, *44* (6), 2022−2028.
(94) Wang, L.; Miao, R.; Wang, X. D.; Lv, Y. T.; Meng, X. R.; Yang, Y. Z.; Huang, D. X.; Feng, L.; Liu, Z. W.; Ju, K. Fouling Behavior of Typical Organic Foulants in Polyvinylidene Fluoride Ultrafiltration Membranes: Characterization from Microforces. *Environ. Sci. Technol.* **2013**, *47* (8), 3708−3714.
(95) Ducker, W. A.; Senden, T. J.; Pashley, R. M. Measurement of Forces in Liquids Using a Force Microscope. *Langmuir* **1992**, *8* (7), 1831−1836.
(96) Newcomb, C. J.; Qafoku, N. P.; Grate, J. W.; Bailey, V. L.; De Yoreo, J. J. Developing a molecular picture of soil organic matter-mineral interactions by quantifying organo-mineral binding. *Nat. Commun.* **2017**, *8*, 396.
(97) Zhai, H.; Wang, L. J.; Putnis, C. V. Molecular-Scale Investigations Reveal Noncovalent Bonding Underlying the Adsorption of Environmental DNA on Mica. *Environ. Sci. Technol.* **2019**, *53* (19), 11251−11259.
(98) Friddle, R. W.; Noy, A.; De Yoreo, J. J. Interpreting the widespread nonlinear force spectra of intermolecular bonds. *Proc. Natl. Acad. Sci. U.S.A.* **2012**, *109* (34), 13573−13578.
(99) Heymann, B.; Grubmuller, H. Dynamic force spectroscopy of molecular adhesion bonds. *Phys. Rev. Lett.* **2000**, *84* (26), 6126−6129.
(100) Merkel, R.; Nassoy, P.; Leung, A.; Ritchie, K.; Evans, E. Energy landscapes of receptor-ligand bonds explored with dynamic force spectroscopy. *Nature* **1999**, *397* (6714), 50−53.
(101) Ridgway, H. F.; Orbell, J.; Gray, S. Molecular simulations of polyamide membrane materials used in desalination and water reuse applications: Recent developments and future prospects. *J. Membr. Sci.* **2017**, *524*, 436−448.
(102) Xiang, Y.; Xu, R.-G.; Leng, Y. How alginate monomers contribute to organic fouling on polyamide membrane surfaces? *J. Membr. Sci.* **2022**, *643*, 120078.
(103) Xiang, Y.; Liu, Y.; Mi, B.; Leng, Y. Molecular Dynamics Simulations of Polyamide Membrane, Calcium Alginate Gel, and Their Interactions in Aqueous Solution. *Langmuir* **2014**, *30* (30), 9098−9106.
(104) Cruz-Silva, R.; Takizawa, Y.; Nakaruk, A.; Katouda, M.; Yamanaka, A.; Ortiz-Medina, J.; Morelos-Gomez, A.; Tejima, S.;

https://doi.org/10.1021/acs.est.3c00414
Environ. Sci. Technol. 2023, 57, 7129−7149

Obata, M.; Takeuchi, K.; Noguchi, T.; Hayashi, T.; Terrones, M.; Endo, M. New Insights in the Natural Organic Matter Fouling Mechanism of Polyamide and Nanocomposite Multiwalled Carbon Nanotubes-Polyamide Membranes. *Environ. Sci. Technol.* **2019**, *53* (11), 6255−6263.
(105) Bi, Y.; Porras, A.; Li, T. Free energy landscape and molecular pathways of gas hydrate nucleation. *J. Chem. Phys.* **2016**, *145* (21), 211909.
(106) Raiteri, P.; Gale, J. D.; Quigley, D.; Rodger, P. M. Derivation of an accurate force-field for simulating the growth of calcium carbonate from aqueous solution: A new model for the calcite− Water interface. *J. Phys. Chem. C* **2010**, *114* (13), 5997−6010.
(107) Raiteri, P.; Gale, J. D. Water is the key to nonclassical nucleation of amorphous calcium carbonate. *J. Am. Chem. Soc.* **2010**, *132* (49), 17623−17634.
(108) Demichelis, R.; Raiteri, P.; Gale, J. D.; Quigley, D.; Gebauer, D. Stable prenucleation mineral clusters are liquid-like ionic polymers. *Nat. Commun.* **2011**, *2* (1), 1−8.
(109) Gale, J. D.; Raiteri, P.; Van Duin, A. C. A reactive force field for aqueous-calcium carbonate systems. *Phys. Chem. Chem. Phys.* **2011**, *13* (37), 16666−16679.
(110) Van Duin, A. C.; Dasgupta, S.; Lorant, F.; Goddard, W. A. ReaxFF: a reactive force field for hydrocarbons. *J. Phys. Chem. A* **2001**, *105* (41), 9396−9409.
(111) Raiteri, P.; Schuitemaker, A.; Gale, J. D. Ion pairing and multiple ion binding in calcium carbonate solutions based on a polarizable AMOEBA force field and ab initio molecular dynamics. *J. Phys. Chem. B* **2020**, *124* (17), 3568−3582.
(112) Byrne, E. H.; Raiteri, P.; Gale, J. D. Computational insight into calcium−sulfate ion pair formation. *J. Phys. Chem. C* **2017**, *121* (46), 25956−25966.
(113) Van Duin, A. C.; Strachan, A.; Stewman, S.; Zhang, Q.; Xu, X.; Goddard, W. A. ReaxFFSiO reactive force field for silicon and silicon oxide systems. *J. Phys. Chem. A* **2003**, *107* (19), 3803−3811.
(114) Fogarty, J. C.; Aktulga, H. M.; Grama, A. Y.; Van Duin, A. C.; Pandit, S. A. A reactive molecular dynamics simulation of the silica-water interface. *J. Chem. Phys.* **2010**, *132* (17), 174704.
(115) Yeon, J.; Van Duin, A. C. ReaxFF molecular dynamics simulations of hydroxylation kinetics for amorphous and nano-silica structure, and its relations with atomic strain energy. *J. Phys. Chem. C* **2016**, *120* (1), 305−317.
(116) Du, T.; Li, H.; Sant, G.; Bauchy, M. New insights into the sol−gel condensation of silica by reactive molecular dynamics simulations. *J. Chem. Phys.* **2018**, *148* (23), 234504.
(117) Demichelis, R.; Schuitemaker, A.; Garcia, N. A.; Koziara, K. B.; De La Pierre, M.; Raiteri, P.; Gale, J. D. Simulation of crystallization of biominerals. *Annu. Rev. Mater. Res.* **2018**, *48*, 327−352.
(118) Sosso, G. C.; Chen, J.; Cox, S. J.; Fitzner, M.; Pedevilla, P.; Zen, A.; Michaelides, A. Crystal nucleation in liquids: Open questions and future challenges in molecular dynamics simulations. *Chem. Rev.* **2016**, *116* (12), 7078−7116.
(119) Zimmermann, N. E.; Vorselaars, B.; Quigley, D.; Peters, B. Nucleation of NaCl from aqueous solution: Critical sizes, ion-attachment kinetics, and rates. *J. Am. Chem. Soc.* **2015**, *137* (41), 13352−13361.
(120) Chakraborty, D.; Patey, G. How crystals nucleate and grow in aqueous NaCl solution. *J. Phys. Chem. Lett.* **2013**, *4* (4), 573−578.
(121) Jiang, H.; Haji-Akbari, A.; Debenedetti, P. G.; Panagiotopoulos, A. Z. Forward flux sampling calculation of homogeneous nucleation rates from aqueous NaCl solutions. *J. Chem. Phys.* **2018**, *148* (4), 044505.
(122) Allen, R. J.; Frenkel, D.; ten Wolde, P. R. Simulating rare events in equilibrium or nonequilibrium stochastic systems. *J. Chem. Phys.* **2006**, *124* (2), 024102.
(123) Li, T.; Donadio, D.; Russo, G.; Galli, G. Homogeneous ice nucleation from supercooled water. *Phys. Chem. Chem. Phys.* **2011**, *13* (44), 19807−19813.
(124) Knott, B. C.; Molinero, V.; Doherty, M. F.; Peters, B. Homogeneous nucleation of methane hydrates: Unrealistic under realistic conditions. *J. Am. Chem. Soc.* **2012**, *134* (48), 19544−19547.
(125) Zimmermann, N. E.; Vorselaars, B.; Espinosa, J. R.; Quigley, D.; Smith, W. R.; Sanz, E.; Vega, C.; Peters, B. NaCl nucleation from brine in seeded simulations: Sources of uncertainty in rate estimates. *J. Chem. Phys.* **2018**, *148* (22), 222838.
(126) Lamas, C.; Espinosa, J.; Conde, M.; Ramírez, J.; de Hijes, P. M.; Noya, E. G.; Vega, C.; Sanz, E. Homogeneous nucleation of NaCl in supersaturated solutions. *Phys. Chem. Chem. Phys.* **2021**, *23* (47), 26843−26852.
(127) Jiang, H.; Debenedetti, P. G.; Panagiotopoulos, A. Z. Nucleation in aqueous NaCl solutions shifts from 1-step to 2-step mechanism on crossing the spinodal. *J. Chem. Phys.* **2019**, *150* (12), 124502.
(128) Gebauer, D.; Cölfen, H. Prenucleation clusters and non-classical nucleation. *Nano Today* **2011**, *6* (6), 564−584.
(129) Wallace, A. F.; Hedges, L. O.; Fernandez-Martinez, A.; Raiteri, P.; Gale, J. D.; Waychunas, G. A.; Whitelam, S.; Banfield, J. F.; De Yoreo, J. J. Microscopic evidence for liquid-liquid separation in supersaturated $CaCO_3$ solutions. *Science* **2013**, *341* (6148), 885−889.
(130) Sebastiani, F.; Wolf, S. L.; Born, B.; Luong, T. Q.; Cölfen, H.; Gebauer, D.; Havenith, M. Water dynamics from THz spectroscopy reveal the locus of a liquid−liquid binodal limit in aqueous $CaCO_3$ solutions. *Angew. Chem., Int. Ed.* **2017**, *56* (2), 490−495.
(131) Henzler, K.; Fetisov, E. O.; Galib, M.; Baer, M. D.; Legg, B. A.; Borca, C.; Xto, J. M.; Pin, S.; Fulton, J. L.; Schenter, G. K.; et al. Supersaturated calcium carbonate solutions are classical. *Sci. Adv.* **2018**, *4* (1), eaao6283.
(132) Beniash, E.; Aizenberg, J.; Addadi, L.; Weiner, S. Amorphous calcium carbonate transforms into calcite during sea urchin larval spicule growth. *Proceedings of the Royal Society of London. Series B: Biological Sciences* **1997**, *264* (1380), 461−465.
(133) Radha, A.; Forbes, T. Z.; Killian, C. E.; Gilbert, P.; Navrotsky, A. Transformation and crystallization energetics of synthetic and biogenic amorphous calcium carbonate. *Proc. Natl. Acad. Sci. U. S. A.* **2010**, *107* (38), 16438−16443.
(134) Rodriguez-Blanco, J. D.; Shaw, S.; Benning, L. G. The kinetics and mechanisms of amorphous calcium carbonate (ACC) crystallization to calcite, via vaterite. *Nanoscale* **2011**, *3* (1), 265−271.
(135) Gebauer, D.; Raiteri, P.; Gale, J. D.; Cölfen, H. On classical and non-classical views on nucleation. *Am. J. Sci.* **2018**, *318* (9), 969−988.
(136) Smeets, P. J.; Finney, A. R.; Habraken, W. J.; Nudelman, F.; Friedrich, H.; Laven, J.; De Yoreo, J. J.; Rodger, P. M.; Sommerdijk, N. A. A classical view on nonclassical nucleation. *Proc. Natl. Acad. Sci. U. S. A.* **2017**, *114* (38), E7882−E7890.
(137) Hu, Q.; Nielsen, M. H.; Freeman, C.; Hamm, L.; Tao, J.; Lee, J.; Han, T. Y.-J.; Becker, U.; Harding, J.; Dove, P.; et al. The thermodynamics of calcite nucleation at organic interfaces: Classical vs. non-classical pathways. *Faraday Discuss.* **2012**, *159* (1), 509−523.
(138) Wang, Y.-W.; Kim, Y.-Y.; Christenson, H. K.; Meldrum, F. C. A new precipitation pathway for calcium sulfate dihydrate (gypsum) via amorphous and hemihydrate intermediates. *Chem. Commun.* **2012**, *48* (4), 504−506.
(139) Van Driessche, A.; Benning, L. G.; Rodriguez-Blanco, J.; Ossorio, M.; Bots, P.; García-Ruiz, J. The role and implications of bassanite as a stable precursor phase to gypsum precipitation. *Science* **2012**, *336* (6077), 69−72.
(140) Stawski, T. M.; Van Driessche, A. E.; Ossorio, M.; Diego Rodriguez-Blanco, J.; Besselink, R.; Benning, L. G. Formation of calcium sulfate through the aggregation of sub-3 nanometre primary species. *Nat. Commun.* **2016**, *7* (1), 1−9.
(141) Aizenberg, J.; Black, A. J.; Whitesides, G. M. Control of crystal nucleation by patterned self-assembled monolayers. *Nature* **1999**, *398* (6727), 495−498.
(142) Takizawa, Y.; Inukai, S.; Araki, T.; Cruz-Silva, R.; Ortiz-Medina, J.; Morelos-Gomez, A.; Tejima, S.; Yamanaka, A.; Obata, M.; Nakaruk, A.; et al. Effective antiscaling performance of reverse-

https://doi.org/10.1021/acs.est.3c00414
Environ. Sci. Technol. 2023, 57, 7129−7149

osmosis membranes made of carbon nanotubes and polyamide nanocomposites. *ACS Omega* **2018**, *3* (6), 6047−6055.
(143) Hudait, A.; Odendahl, N.; Qiu, Y.; Paesani, F.; Molinero, V. Ice-nucleating and antifreeze proteins recognize ice through a diversity of anchored clathrate and ice-like motifs. *J. Am. Chem. Soc.* **2018**, *140* (14), 4905−4912.
(144) Qiu, Y.; Hudait, A.; Molinero, V. How size and aggregation of ice-binding proteins control their ice nucleation efficiency. *J. Am. Chem. Soc.* **2019**, *141* (18), 7439−7452.
(145) Liu, K.; Wang, C.; Ma, J.; Shi, G.; Yao, X.; Fang, H.; Song, Y.; Wang, J. Janus effect of antifreeze proteins on ice nucleation. *Proc. Natl. Acad. Sci. U. S. A.* **2016**, *113* (51), 14739−14744.
(146) Eickhoff, L.; Dreischmeier, K.; Zipori, A.; Sirotinskaya, V.; Adar, C.; Reicher, N.; Braslavsky, I.; Rudich, Y.; Koop, T. Contrasting behavior of antifreeze proteins: Ice growth inhibitors and ice nucleation promoters. *J. Phys. Chem. Lett.* **2019**, *10* (5), 966−972.
(147) Phan, A.; Bui, T.; Acosta, E.; Krishnamurthy, P.; Striolo, A. Molecular mechanisms responsible for hydrate anti-agglomerant performance. *Phys. Chem. Chem. Phys.* **2016**, *18* (36), 24859−24871.
(148) Naullage, P. M.; Bertolazzo, A. A.; Molinero, V. How do surfactants control the agglomeration of clathrate hydrates? *ACS Central Science* **2019**, *5* (3), 428−439.
(149) Freger, V.; Gilron, J.; Belfer, S. TFC polyamide membranes modified by grafting of hydrophilic polymers: an FT-IR/AFM/TEM study. *J. Membr. Sci.* **2002**, *209* (1), 283−292.
(150) Kim, N.; Shin, D. H.; Lee, Y. T. Effect of silane coupling agents on the performance of RO membranes. *J. Membr. Sci.* **2007**, *300* (1−2), 224−231.
(151) Shafi, H. Z.; Matin, A.; Akhtar, S.; Gleason, K. K.; Zubair, S. M.; Khan, Z. Organic fouling in surface modified reverse osmosis membranes: Filtration studies and subsequent morphological and compositional characterization. *J. Membr. Sci.* **2017**, *527*, 152−163.
(152) Kharraz, J. A.; An, A. K. Patterned superhydrophobic polyvinylidene fluoride (PVDF) membranes for membrane distillation: Enhanced flux with improved fouling and wetting resistance. *J. Membr. Sci.* **2020**, *595*, 117596.
(153) Zhao, F.; Ma, Z.; Xiao, K.; Xiang, C.; Wang, H.; Huang, X.; Liang, S. Hierarchically textured superhydrophobic polyvinylidene fluoride membrane fabricated via nanocasting for enhanced membrane distillation performance. *Desalination* **2018**, *443*, 228−236.
(154) Jaramillo, H.; Boo, C.; Hashmi, S. M.; Elimelech, M. Zwitterionic coating on thin-film composite membranes to delay gypsum scaling in reverse osmosis. *J. Membr. Sci.* **2021**, *618*, 118568.
(155) Karanikola, V.; Boo, C.; Rolf, J.; Elimelech, M. Engineered slippery surface to mitigate gypsum scaling in membrane distillation for treatment of hypersaline industrial wastewaters. *Environ. Sci. Technol.* **2018**, *52* (24), 14362−14370.
(156) Su, C.; Horseman, T.; Cao, H.; Christie, K.; Li, Y.; Lin, S. Robust superhydrophobic membrane for membrane distillation with excellent scaling resistance. *Environ. Sci. Technol.* **2019**, *53* (20), 11801−11809.
(157) Liu, L.; Charlton, L.; Song, Y.; Li, T.; Li, X.; Yin, H.; He, T. Scaling resistance by fluoro-treatments: the importance of wetting states. *Journal of Materials Chemistry A* **2022**, *10* (6), 3058−3068.
(158) Xiao, Z. C.; Li, Z. S.; Guo, H.; Liu, Y. J.; Wang, Y. S.; Yin, H. B.; Li, X. M.; Song, J. F.; Nghiem, L. D.; He, T. Scaling mitigation in membrane distillation: From superhydrophobic to slippery. *Desalination* **2019**, *466*, 36−43.
(159) Lin, N. H.; Kim, M. M.; Lewis, G. T.; Cohen, Y. Polymer surface nano-structuring of reverse osmosis membranes for fouling resistance and improved flux performance. *J. Mater. Chem.* **2010**, *20* (22), 4642−4652.
(160) Qi, Y.; Tong, T.; Zhao, S.; Zhang, W.; Wang, Z.; Wang, J. Reverse osmosis membrane with simultaneous fouling-and scaling-resistance based on multilayered metal-phytic acid assembly. *J. Membr. Sci.* **2020**, *601*, 117888.
(161) Hao, Z.; Zhao, S.; Li, Q.; Wang, Y.; Zhang, J.; Wang, Z.; Wang, J. Reverse osmosis membranes with sulfonate and phosphate groups having excellent anti-scaling and anti-fouling properties. *Desalination* **2021**, *509*, 115076.
(162) Mankol, V.; Hao, Z.; Zhao, S.; Wu, H.; Qi, Y.; Wang, Z.; Wang, J. Sulfonated Reverse Osmosis Membrane Fabricated with Comonomer Having Excellent Scaling and Fouling Resistance. *Ind. Eng. Chem. Res.* **2021**, *60* (7), 3095−3104.
(163) Wang, S.; Mu, C.; Xiao, K.; Zhu, X.; Huang, X. Surface charge regulation of reverse osmosis membrane for anti-silica and organic fouling. *Sci. Total Environ.* **2020**, *715*, 137013.
(164) Xiao, Z.; Zheng, R.; Liu, Y.; He, H.; Yuan, X.; Ji, Y.; Li, D.; Yin, H.; Zhang, Y.; Li, X.-M.; et al. Slippery for scaling resistance in membrane distillation: A novel porous micropillared superhydrophobic surface. *Water Research* **2019**, *155*, 152−161.
(165) Liu, L.; Xiao, Z.; Liu, Y.; Li, X.; Yin, H.; Volkov, A.; He, T. Understanding the fouling/scaling resistance of superhydrophobic/omniphobic membranes in membrane distillation. *Desalination* **2021**, *499*, 114864.
(166) Anis, S. F.; Hashaikeh, R.; Hilal, N. Reverse osmosis pretreatment technologies and future trends: A comprehensive review. *Desalination* **2019**, *452*, 159−195.
(167) Venkatesan, A. *Ion exchange pretreatment for reverse osmosis desalination of brackish water*. Master Thesis, Purdue University, 2010.
(168) Apell, J. N.; Boyer, T. H. Combined ion exchange treatment for removal of dissolved organic matter and hardness. *Water Res.* **2010**, *44* (8), 2419−2430.
(169) Pérez-González, A.; Ibáñez, R.; Gómez, P.; Urtiaga, A. M.; Ortiz, I.; Irabien, J. A. Recovery of desalination brines: separation of calcium, magnesium and sulfate as a pre-treatment step. *Desalination and Water Treatment* **2015**, *56* (13), 3617−3625.
(170) Levchuk, I.; Màrquez, J. J. R.; Sillanpää, M. Removal of natural organic matter (NOM) from water by ion exchange−a review. *Chemosphere* **2018**, *192*, 90−104.
(171) Comstock, S. E.; Boyer, T. H. Combined magnetic ion exchange and cation exchange for removal of DOC and hardness. *Chem. Eng. J.* **2014**, *241*, 366−375.
(172) Hakizimana, J. N.; Gourich, B.; Vial, C.; Drogui, P.; Oumani, A.; Naja, J.; Hilali, L. Assessment of hardness, microorganism and organic matter removal from seawater by electrocoagulation as a pretreatment of desalination by reverse osmosis. *Desalination* **2016**, *393*, 90−101.
(173) Zhang, X.; Lu, M.; Idrus, M. A. M.; Crombie, C.; Jegatheesan, V. Performance of precipitation and electrocoagulation as pretreatment of silica removal in brackish water and seawater. *Process Saf. Environ. Prot.* **2019**, *126*, 18−24.
(174) Ho, J. S.; Ma, Z.; Qin, J.; Sim, S. H.; Toh, C.-S. Inline coagulation−ultrafiltration as the pretreatment for reverse osmosis brine treatment and recovery. *Desalination* **2015**, *365*, 242−249.
(175) Subramani, A.; Schlicher, R.; Long, J.; Yu, J.; Lehman, S.; Jacangelo, J. G. Recovery optimization of membrane processes for treatment of produced water with high silica content. *Desalination and Water Treatment* **2011**, *36* (1−3), 297−309.
(176) Liu, W.; Liu, B.; Li, X. UV/Fe (II) synergistically activated S (IV) per-treatment on HA-enhanced Ca2+ scaling in NF filtration: Fouling mitigation, mechanisms and correlation analysis of membrane resistance in different filtration stage. *Chemosphere* **2022**, *308*, 136302.
(177) Yin, Y.; Li, T.; Zuo, K.; Liu, X.; Lin, S.; Yao, Y.; Tong, T. Which Surface Is More Scaling Resistant? A Closer Look at Nucleation Theories for Heterogeneous Gypsum Nucleation in Aqueous Solutions. *Environ. Sci. Technol.* **2022**, *56* (22), 16315−16324.
(178) Ang, W. S.; Elimelech, M. Protein (BSA) fouling of reverse osmosis membranes: implications for wastewater reclamation. *J. Membr. Sci.* **2007**, *296* (1−2), 83−92.
(179) Lee, S.; Ang, W. S.; Elimelech, M. Fouling of reverse osmosis membranes by hydrophilic organic matter: implications for water reuse. *Desalination* **2006**, *187* (1−3), 313−321.
(180) Zhao, X.; Wu, Y.; Zhang, X.; Tong, X.; Yu, T.; Wang, Y.; Ikuno, N.; Ishii, K.; Hu, H. Ozonation as an efficient pretreatment method to alleviate reverse osmosis membrane fouling caused by

https://doi.org/10.1021/acs.est.3c00414
Environ. Sci. Technol. 2023, 57, 7129−7149

complexes of humic acid and calcium ion. *Front. Environ. Sci. Eng.* **2019**, *13*, 1−12.
(181) Liu, L.; He, H.; Wang, Y.; Tong, T.; Li, X.; Zhang, Y.; He, T. Mitigation of gypsum and silica scaling in membrane distillation by pulse flow operation. *J. Membr. Sci.* **2021**, *624*, 119107.
(182) Yu, W.; Song, D.; Chen, W.; Yang, H. Antiscalants in RO membrane scaling control. *Water Res.* **2020**, *183*, 115985.
(183) Weijnen, M.; Van Rosmalen, G. The influence of various polyelectrolytes on the precipitation of gypsum. *Desalination* **1985**, *54*, 239−261.
(184) Gebauer, D. How can additives control the early stages of mineralisation? *Minerals* **2018**, *8* (5), 179.

https://doi.org/10.1021/acs.est.3c00414
Environ. Sci. Technol. 2023, 57, 7129−7149